scientific reports

Check for updates

OPEN

Functionalization of biochar using SDS/SAP nanomicelles enhanced its immobilization capacity for dyes and heavy metals in water

Kun Tian[1,2], Chunping Li[1,2], Huiming Liu[1] & Lianchun Wang[1,2]✉

To enhance the adsorption capacity of biochar (BC), herein a novel multifunction modified biochar (SDMBC) was prepared by directly crosslinking of the nanomicelle of sodium dodecyl sulfate/ sapindus-saponin (SDS/SAP) composite system onto the BC through a simple, environmental friendly approach. Result showed that the adsorption performance of SDMBC has been greatly improved, compared with BC or using alone SDS and SAP, adsorption ability increased by 48.83%, 29.50%, 36.44%, respectively, the best modified effect was appeared when the concentration of SAP to SDS was 0.8 and 0.8 CMC. SDMBC exhibited high adsorption abilities of 130.23, 108.43, 277.09 125.27, 112.78 mg/g for heavy metal ions lead Pb(II), Cadmium Cd(II) and organic pollutants with different chemical properties bisphenol A(BPA), Methylene blue (MB), P-nitrophenol (PNP), respectively, higher than most previously reported adsorbents, importantly, SDMBC can still efficient removal capabilities even in the binary competition. Subsequently, the SDMBC and BC was characterized by Fourier Transform infrared spectroscopy (FT-IR), X-ray diffraction (XRD), scanning electron microscopy (SEM), Zeta potential (Zeta), it found SDMBC has a more layered structure, richer functional groups and more amorphous structure compared with BC, which are closely related with improving its adsorption capacity. The adsorption behavior of SDMBC for MB show that process was found to be spontaneous, propitious, endothermic, the adsorption isotherms fitted Freundlich models well, pseudo-second-order best describes kinetics adsorption, suggesting that the process is multi-layer chemical adsorption. The little affected by ionic strength and coexisting substances, could remained removal rate over a wide pH range, SDMBC still keep high removal rates even after 5 reuses. Based on FT-IR analysis, plausible adsorption mechanism proposed, including hydrogen bond, electrostatic attraction and π-π bonding. Cost analysis manifests that the SDMBC are high efficiency and cheap eco-adsorbents compared with commercial activated carbon, and the SDMBC dosage required for the removal of 99% of a fixed amount of MB in different volumes of effluent was predicted. Seven machine learning (ML) models were used to predict the MB (60 mg/L) adsorption of the SDMBC, using Shapley Additive Explanations (SHAP) for model interpretation. Finding Extreme Gradient Boosting (XGBoost) exhibited best performance, the order of feature importance as time> Ratio> pH> concentration> temperature. Thus, SDMBC as a new cheap and eco-adsorbents, can be used to effectively remove various types of pollutants, has a great application potential in sewage treatment, while the accurate ML prediction model presented a valuable advice for designing efficient adsorbents and optimization operating conditions in the future.

Keywords Micellar aggregates, Modification, Heavy metal, Organic pollutant, Machine learning

With the rapid development of industry over the past decades, an increasing number of toxic substances were discharge into ecological environment, contributing to many serious environmental problems, such as water and soil pollution[1]. Among them, organic pollutants (OP) and heavy metal ions (HMs) are one of the most common and harmful pollutants. Among various HMs, Cd(II) and pb(II) are the most common pollutants in

[1]Key Laboratory for Forest Resources Conservation and Utilization in the Southwest Mountains of China, Ministry of Education, Southwest Forestry University, Kunming 650224, Yunnan, China. [2]College of Forestry, Southwest Forestry University, Kunming 650224, Yunnan, China. ✉email: 1390498843@qq.com

wastewater, entered the environmental from industrial effluents. Unfortunately, Cd(II) and pb(II) are highly toxic and carcinogenic and can cause serious harm for human health, even in trace amounts[2].

Phenols and dyes also are one of the most poisonous and common OP, generally speaking, various OP usually coexisting in the polluted water, effective purification water pose a great challenge due to their different physical and chemical properties. From example, water-insoluble bisphenol A (BPA) an endocrine disruptor with genotoxic and potentially carcinogenic widely used as flame retardant in fabric production, it often coexists with other water-soluble dye such as Methylene blue (MB)[3]. MB is a typical cationic organic dye frequently used in textile and food processing, which can cause serious ecological problems and harm human healthy. P-nitrophenol (PNP), a very common coexisting substance in dye wastewater, it are commonly used in plastic, leather, dyes industries[4], moreover, PNP is an organic phenolic compound with highly destructive of living organism, listed as priority pollutant. Thus, removing those toxic substances from the environment has important significant to ensure human health and maintain ecological environmental security[5].

Nowadays, various advanced technologies had been developed to for OP and HMs removal from wastewater, like advanced oxidation, adsorption, biodegradation, photocatalytic degradation. The adsorption method widely used because its low cost, simple operation and high efficiency. among, activated carbon is the most commonly used adsorbents, but, it disadvantage, complex and expensive preparation process also limits its application. BC are increasingly becoming the focus of scientific disciplines due to advantage of low cost, beneficial environmental applications, meanwhile, the cost of activated carbon (1500 dollars per ton) was 6 times of BC (246 dollars per ton)[5], thus, currently, BC as is an alternative to activated carbon has been used to removal multiple pollutant from waster water.

In recent years, the use of agricultural forestry waste as bio-adsorbents for removal pollutant was focused because of its cost effective and eco-friendliness, but, owing to poor adsorption properties, their are usually activated and modified enhance their adsorption capacity[6]. Converting their into BC is the most commonly activation method. Unfortunately, the preparation BC requires high temperature, but high temperature will cause the degradation of the active functional groups, such as hydroxyl, carboxylic and ether groups[7], which makes it uniquely improper for application to adsorption of pollutants. One of the most effective methods for improving adsorption capacity adsorbent is by introducing appropriate functional groups, including chemical and physical modification[8]. Although acid modification (e.g., nitric acid, phosphoric acid) could increase abundance oxygen-containing functional groups, it has the disadvantage of low specific surface area and poor hydrophilicity[9]. While, modification with alkaline solutions (like sodium hydroxide and potassium hydroxide) increases the specific surface area, the hydrophilicity of the BC is reduced[10]. What is worse, the use of large amount of traditional inorganic acids or alkalis not only increased the cost, but also causes secondary pollution could even raise serious environmental problems, did not comply with the principles sustainability green chemistry.

Moreover, as a novel chemical modification technology, surfactants are increasingly considered as a promising ways to enhance the adsorption performance of BC[11], because surfactant modification can improve the dispersion of BC in solution, enhance the affinity between BC and solution water, and improve the adsorption characteristics of the surface of BC[12]. Meanwhile, the surfactant can alter the character of charges on the BC surface and introduce more active functional groups, which can more provide ion exchange and binding-site for contaminants[13], Surfactant has the advantages of less damage to the structure of BC, which is clearly advantageous is introduce suitable functional groups while retaining original structure adsorbent. Importantly, using surfactants for adsorbents modification in the preparation process is mature, the raw materials are easily available and inexpensive, also we chose biodegradable surfactant SDS, natural surfactants SAP and thus minimizing the environmental pollution. Thus, the excellent activity of surfactants making them an increasingly popular choice for enhancing adsorbent[14].

Also, it should be noted, there are still a number of disadvantages when using the surfactant individually, such as, the anionic surfactants are easily forms precipitate in the soil, and nonionic surfactants are likely to adsorb onto the fractions of soil[15], indeed, numerous studies have shown the problem can be solved using the different surfactants are mixed use, for instance, using a combination of nonionic with anionic surfactants could be prevented sorption of nonionic surfactants[16]. Furthermore, the surfactants were mixed use is able to achieve "1 + 1 = 2" effects, and also, compared with single surfactant, mixed surfactants are capable of lowering Critical Micelle Concentration (CMC) of surfactant[17], and it have synergistic advantage in micelles are created and solubilized, and can use over a broader range of salinity, hardness, temperature and stronger ordering of the core of the micelles within the surfactants[18].

SDS is an anionic surfactant with biodegradable, it have alkyl chains and ionizes to produce negative charge in water. Previous research show that the modification of SDS could improve the adsorption capacity of the BC for OP, particularly cationic dyes, such as MB[19]. Li et al. prepared SDS-B beads through double-network hydrogel beads modification SDS, resulting in enhanced adsorption capacity and hydrophobicity[20]. Lee et al. a functionalized biochar (MFB) was prepared by supporting mg and Fe onto sawdust BC (SB), thereafter, the SDS solution was mixed with MFB to synthesize the organic BC (MSB), the surface roughness, aromaticity, and hydrophobicity of MSB is significantly improved compared to SB, MSB exhibited a high adsorption capacity for Pb(II) (405.2 mg/g) and Cd(II) (673 mg/g)[21].These results indicate that the modification of SDS could greatly improve the adsorption capacity of the sorbents for OP and HMs.

SAP is a non-ionic biosurfactant, which derived from *Sapindus mukorossi Gaertn*, it has many advantages including biodegradability, low toxicity and low critical micelle (about one-tenth of synthetic surfactant), and can be mass-production with low cost[22]. In addition, SAP have of a large amount of active functional groups (AFG) including hydroxyl, carbon-carbon double-bond, aldehyde, epoxy, aromatic ring and carboxyl[23], which can form strong interactions with OP, such as hydrogen bond, π-π interaction and electrostatic attraction[19,24], thus, the performance of sorbents through SAP modified is usually superior to the parent sorbents. For example,

Kurniawan et al. used surfactant(SAP)extracted from the plant sapindus to improved the performance of the adsorbent. the showed that the utilization of SAP is successful in enhancing the capacity of the adsorbent for MB[14].

Moreover, these AFG confers to SAP with remarkable ability to capture of HMs, because of AFG can form stable complexes with HMs by strong complexation. Importantly, relevant research shows that the SAP complexing ability toward HMs comparable to inorganic acid and even higher than chelating agent[25]. For instance Mondal et al. extracted a natural surfactant (SAP) from the plant Sapindus mukorossi and demonstrated SAP effectiveness in removing chromium from water[26]. Gao et al.[27], Huang et al.[28] and Chen et al.[29] observed that SAP has a strong ability to form complexes with these HMs. These studies demonstrated the effectiveness and prospect of the SAP modification in enhancing the performance of the adsorbents for removing HMs.

What is more interesting, SAP and SDS as surfactants, a polar hydrophilic groups at one end and non-polar hydrophilic groups at other end, they can self-assemble into micelle-like aggregates[23], this micellar nanostructures expected to provide more active site for pollutants, and can encapsulated OP into its hydrophobic core via hydrophobic interaction between surfactant amphiphilic structure and OP.

Hence, it is reasonable to conjecture that using dual surfactant (SDS/SAP) micelles synergistic effect in to modify BC, can greatly strengthen the interaction between the various pollutants and BC, thereby improving adsorption efficiency and selectivity of pollutants, moreover, the presence of anionic surfactant enhanced the electrostatic attraction force between adsorbents and cationic pollutants, can overcome the low removal efficiency of other materials under alkaline conditions[30]. Although there are has been some research on the removal pollutants by used surfactant modified BC, but, these studies usually focus on single surfactant modification, or compare the modification performance different types surfactants. To the best of our knowledge, there is still a lack of high-quality research on micelles of dual surfactant (biodegradable) as modifier to strengthen adsorption performance of BC, especially, application in simultaneously removal organic pollutants (OP) with different electrochemical properties, and heavy metal (HMs) has not yet been reported, which greatly limits mixed micelles application in the development adsorbents with versatile and high adsorption capacity, and to lay a theoretical foundation for find an environmentally-friendly, cheap and efficient reagents replace organic acids, inorganic acids et al. chemical reagents.

Adsorption is an extremely complex process, the removal efficiency is affected by the physicochemical properties of adsorbents and target pollutants, and the adsorption conditions such as pH, temperature, initial concentration, time and dosage. Although adsorption kinetics and adsorption isotherms can explain adsorption behavior, but they shortcomings include time-consuming and may only consider for certain factors[31].

ML is a powerful and emerging method to illustrate complex multivariate relationship illustrate, by creating mapping function based on data. ML can adaptively learns how create mapping function from input to output data without knowing mathematical relationships between them, therefor, ML can avoid the shortcoming of classical formulation to a certain extent[32]. What more important, it can analyze the non-linear relationship many characteristic variables influencing adsorption properties, explain hidden relationships, predictive performance, can greatly reduce cost and time of experimental, given that, ML have been widely used in design screening adsorbent, construction of adsorption, optimization of adsorption parameters[33]. However, report on is still very lacking presently, using ML to establish predictive models to predict the adsorption capacity and optimization adsorption process for MB, more, previous works on the preparation of MB has usually emphasized on high performance, but, based on different application scenarios to carry out targeted operation parameters and preparation process often ignored, this mean that the achieve efficient removal is very difficult under different application conditions, hence, leverage ML to advices for adsorption parameters and preparation process offer a workable solution to this problem.

Here, a new adsorbent SDMBC, with good overall performance and high adsorption capacity was prepared use a simple and efficient modification method, the dual surfactant (SDS/SAP) self-assembled nanomicelles directly crosslinked onto surface of BC. SDMBC and BC were characterized by FTIR, SEM, XRD and Zeta. The effect of pH, molar ratio of SDS/SAP, initial concentration, ionic strength were investigated. Adsorption kinetics, isotherm, thermodynamics and mechanism of SDMBC for MB were comprehensively analysed, and the reusability of SDMBC was explored. Then, the seven ML were employed to build prediction models and performance evaluation are performed, moreover, using Shapley Additive Explanation to analyse for feature importance to expound the relationship between the input and output variables. Subsequently, the HMs (pb(II), Cd(II)) and the OP with different electrochemical properties and structure (PNP, BPA, MB) was chosen as model pollutant, to evaluate SDMBC adsorption capacity under both single and binary systems, this comprehensive approach highlights the effectiveness and novelty and of our work.

Materials and methods

Materials

Sapindus fruit (SPF) was purchased from a state Forest Farm near Kunming of Yunnan province. Sapindus-saponins (SAP, 99%) was bought from Xi'an Shouhe Biotechnology Co., LTD. Hydrochloric acid (HCl), sulfuric acid (H_2SO_4), sodium chloride (NaCl), sodium bicarbonate ($NaHCO_3$), sodium hydroxide (NaOH) and calcium chloride ($CaCl_2$) were obtained from Shanghai Aladdin Bio-Chem Technology Co., LTD. P-nitrophenol (PNP), bisphenol A (BPA), methylene blue (MB), Lead chloride ($pbcl_2$) and cadmium nitrate ($Cd(NO_3)_2$) were supplied by Tianjin windship Chemical Reagent Technology Co., LTD. All chemical reagents are analytical grade.

Preparations

Synthesis of BC

The hulled SPF were shatter to extract the hard shell, and its were ground to 250 μm, other impurities were removed by further rinsing with deionized water, then clean sample were dried to constant mass at 308 K. Then,

about 20 g of dry sample was put in a porcelain crucible and sealed in a quartz tube reactor, thereafter, the quartz tube reactor installed on the electric furnace. Temperature of the furnace were heated from room temperature to 778 K at the heating rate 10 ℃ per minute under nitrogen protection (nitrogen flow rate was 300 mL per minute), then held at maximum temperature (778 K) for 3 h. Finally, the electric furnace was cooled to room temperature naturally, the resulting products were collected. Prior to surface modification dilute nitric acid bath was used to remove the impurities of biochar, and washed again with distilled water until the pH was neutral.

Synthesis of SDMBC

200, 500, 800, 1000, 2000 mg SAP and 461.4, 1154, 1845, 2307, 4614 mg SDS were added in 1000 mL distilled water to prepare 0.2 + 0.2, 0.5 + 0.5, 0.8 + 0.8, 1 + 1, 2 + 2 CMC SAP/SDS solutions, respectively. Moreover, 800 and 1845 mg of SAP and SDS is dispersed in 1000 mL of distilled water to prepare 0.8 CMC SAP and SDS solutions, respectively. Subsequently, 250 mL SAP/SDS solution (the concentration of 0.8 + 0.8 CMC or other concentration required) was added to a 500 mL conical bottle, then, add 5 g of BC, the mixture was stirred (220 rpm/min) for 12 h at 338 K, after that allowed to settle for 1 h, and the supernatant was discarded, the adsorbents obtained were dried at 383 K. The schematic illustration of SDMBC preparation is shown in Fig. 1.

Characterization

The SDMBC and BC was characterized by Fourier transform infrared instrument (FTIR, Thermo Scientific Nicolet iN10), scanning electron microscopy (SEM, TESCAN MIRA LMS), X ray diffraction (XRD, Rigaku Ultima IV X) and zeta potentials analysis (Zeta, Malvern Zetasizer Nano ZS9).

Batch experiments

Factors including pH, SDS/SAP Ratio, concentration, ionic strength, and coexisting substances this effect on the adsorption performance was researched. For detailed experimental procedures, adsorption isotherm, adsorption kinetics, thermodynamic parameters models, please see Supplementary Materials 3 (Sect. 2.4.1 to 2.4.6).

Construction of ML models

In this study, seven ML methods, such as PF, BP, CNN, SVR, AdaBoost, LsBoost and XGBoost, were employed to build a predictive model, the input date were transformed using Eq. (1) to normalized before building modes[34]. Please see the Supplementary Material 1 for a formal introduction and method of the seven model.

$$Y = \frac{x - x_{min}}{x_{max} - x_{min}} \tag{1}$$

Y*: normalized value of x, x: original eigenvalue, x_{min}: minimum value of x, x_{max}: maximum value of x.

Performance evaluation of ML

The performance of all models was evaluated using coefficient of determination (R^2), root mean square error (RMSE) and mean absolute error (MAE) were calculated by Eqs. (2), (3) and (4)[31], respectively. All machine

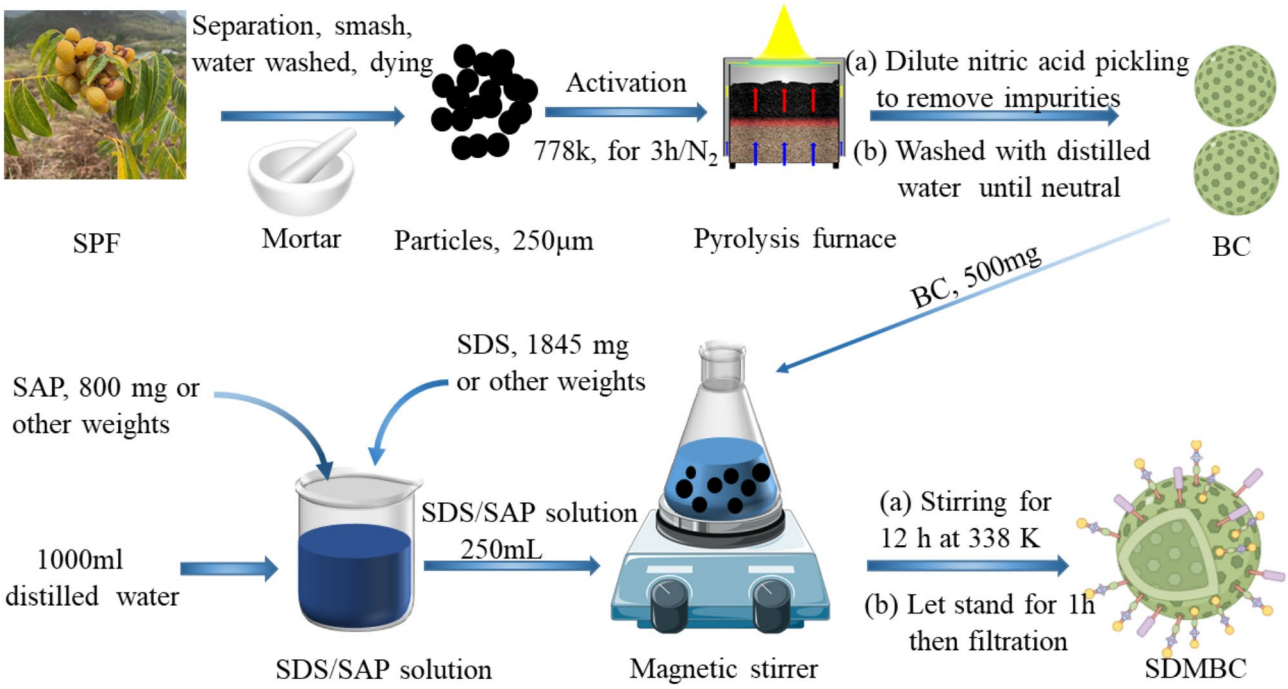

Fig. 1. Preparation of SDMBC.

learning were performed using Matlab (2022b), all sample were randomly divided into a training set (0.8) and a test set (0.2).

$$R^2 = 1 - \frac{\sum_{i=1}^{n}(y_i - x_i)^2}{\sum_{i=1}^{n}(y_i - y)^2} \quad (2)$$

$$RMSE = \sqrt{\frac{1}{N}\sum_{i=1}^{N}(y_i - x_i)^2} \quad (3)$$

$$MAE = \frac{1}{N} \times \sum_{i=1}^{N} |y_i - x_i| \quad (4)$$

Where n: total number of samples, y_i: true value, x_i: prediction value, y: the mean of the true values.

Results and discussion

Characterization of SDMBC and BC

FT-IR analysis

For the purpose of investigative the surface functional groups on BC change between pre-and post-modification, which were characterized with FT-IR (Fig. 2). The band of SDMBC at 1573 cm^{-1} and 1803 cm^{-1} were assigned to COOH, stretching vibration band of C-O of carboxylic appeared at 1028 cm^{-1} vibration, this corresponds to SAP contained substantial amounts of carboxyl, the band at 1471 cm^{-1}, 1157 cm^{-1} and 1064 cm^{-1} corresponding to CH_2, S=O and sulfonate asymmetric stretching vibrations of SDS[35], respectively. The adsorption band of BC at 3420 cm^{-1},1625 cm^{-1},1270 cm^{-1} and 1118 cm^{-1} broad peak are attribute to OH stretching vibration, C=O

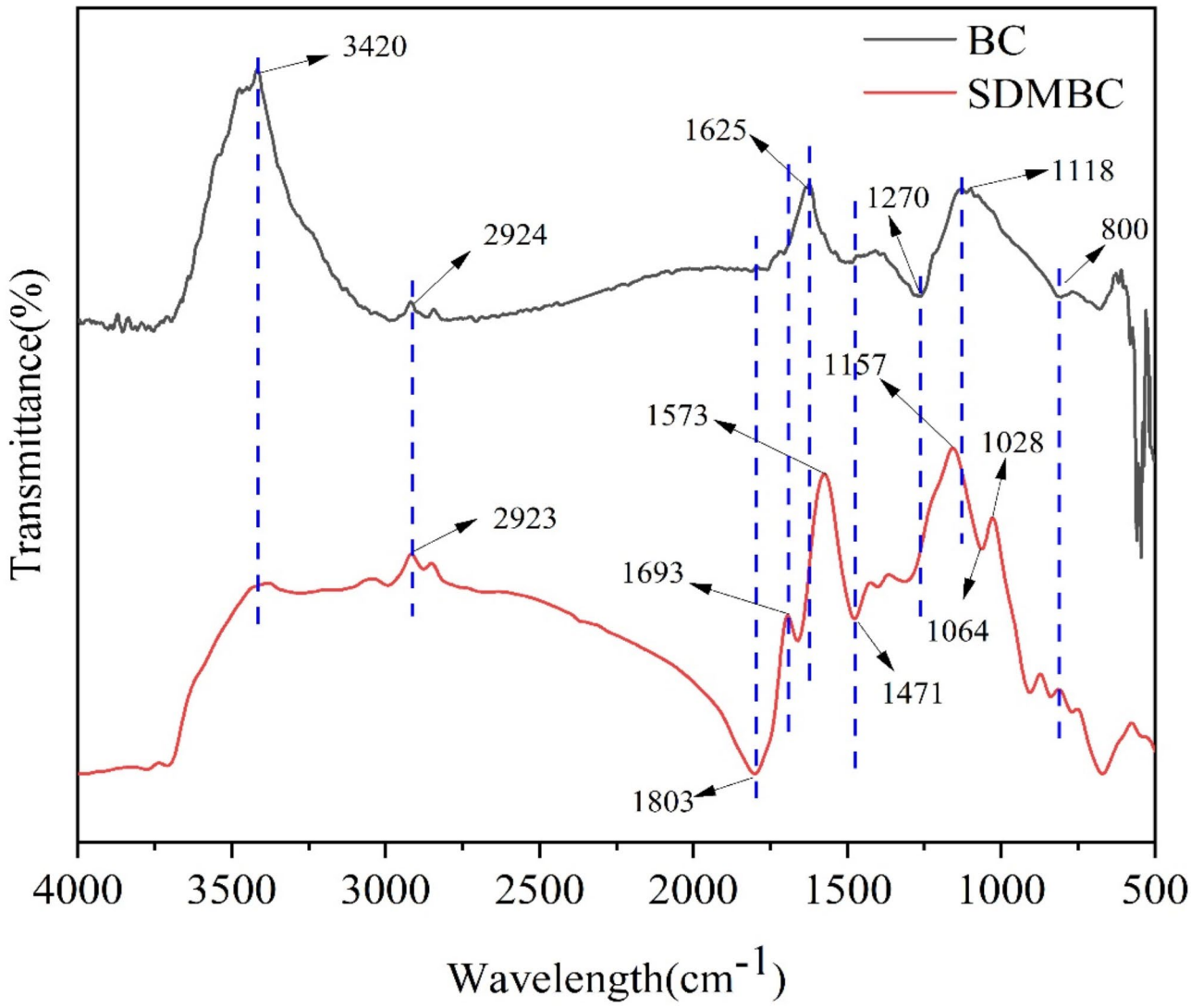

Fig. 2. FT-IR spectra of BC and SDMBC.

symmetric vibrations of carboxylic acids and C=C of aromatic rings and C-O vibration, respectively, moreover, the region below 800 cm^{-1} in both spectra represented to C-H bending variation in aromatic nucleus.

There was several obvious FT-IR spectra changes in SDMBC compared to BC. Firstly, the diffraction peaks corresponding to hydroxyl (3400 cm^{-1}) phases were basically disappeared after modification, this could be caused by BC hydroxyl is hydrogen bonded to hydroxyl groups of modifier during the modification process, which is also the main reason the SDS/SAP molecules were loaded of firmly to the BC. Secondly, the appearance of the new peak at 1471 cm^{-1}, 1157 cm^{-1}, 1064 cm^{-1} and 1028 cm^{-1}, 1064 cm^{-1}, which indicated that modifier was loaded successfully. After modification, the peak at 1270 cm^{-1} corresponded vibrations of C=C bonds in the benzene ring disappear, this may be related to the π-π bonds establish between benzene rings on the surface of BC and SAP/SDS molecule via π-π coupling. The flexural vibrational peak of C-O at 1118 cm^{-1} was weakened, while new diffraction peaks were found at 1517 cm^{-1}, indicating SDMBC has richer carboxylate groups compared to BC[36]. Thirdly, the peak of adsorption in the wavelength range of 1625 cm^{-1}~1804 cm^{-1} corresponding to COOH bending vibrations, the intensity of absorption peak in this area is obviously enhanced after modification, indicating the SDMBC has more carboxyl than BC, based on previous researches, the increase of carboxyl group content is beneficial to the adsorption of pollutants[37]. Similarly, SDMBC have more free oxygen-containing functional groups make it excellent dispersibility in water, which are conducive to its adsorption of pollutants in aqueous solution[12]. Finally, the region below 800 cm^{-1} diffraction peaks was significantly weakened, this can be attributed to the peak for aromatic C–H stretching were occupied by SDS/SAP molecular, this also further demonstrated that SDS/SAP was successfully assembled to BC[38].

XRD analysis

From Fig. 3, it can see that the carbon structure of SDMBC and BC exist mainly in the form of amorphous with the presence of a few crystals, and both have similar diffraction peaks, suggesting that the SDS/SAP modified did not cause obvious destroy to BC structure. Specifically, a broad with high intensity X-ray diffraction peaks is observed around $2\theta = 23°$ in both samples, corresponding to the (002) plane of graphite, which mainly triggered by amorphous structure consisting of graphene sheets[39]. Meanwhile, the diffraction peak from SDMBC at $2\theta = 23°$ was obviously weaken relative to the BC, indicating that SAP/SDS modification has corrosive weak effect on BC structure, this may be caused by voids are form from are covered graphene surface by micelles formed with modifier. In addition, a very weak diffraction peak around at $2 = 43°$ in the diffraction peak of BC, which correspond to an amorphous structure composed of randomly oriented aromatic graphene, however, this peak almost disappears in SDMBC, this can be attributed to the complex of micelles was formed on graphene, but, this can increase the specific surface area and exposed the chemical bond out, which help improve the adsorption capacity of SDMBC. Moreover, the BC displays a weak diffraction peak at 51° and 61°, whereas after the modification process, the corresponding peaks almost disappeared, this is probably because SDS/SAP micelles formed a complex with BC. Finally, SDMBC exhibits smoother diffraction peak, suggesting that it has large amorphous morphology compare with the BC, this is beneficial to adsorption[40]. Anbia pointed out that the XRD diffraction peak intensity show a rather strong decreasing trend nanoporous carbon after modification with SDS[41], these research results are strikingly similar to our conclusion.

SEM analysis

The surface morphology of BC and SDMBC were depicted by SEM. For BC, the SEM image (Fig. 4a) see clearly the rolled-up edge, the smooth and wrinkled surface morphology and irregular lamellar structure with some macroporous structure. For SDMBC (Fig. 4b), the surface became rough, part pore structure were occupied by modifier, but, the lamellar structures was reinforced on BC surface, likely due mixed micelles covered the BC surface, this can provide more surface sites for pollutants. Furthermore, the morphology of pore structure was further observed, the internal pore structure of BC is relatively smooth and existing with a small number of small particles (Fig. 4c), while, the internal part of SDMBC pore structure were are occupied by modifier molecules, become rough, there was a large number of white crystal particles (Fig. 4d), which can provide more active functional groups and adsorption sites for pollutants.

Zeta analysis

In order to study the surface charge distribution of SDMBC, the zeta potentials of SDMBC were measured in a pH range of 3.0–11.0. As expected, the zeta potential values is retentively negative of SDMBC within the range from 3 to 11 (Fig. 5), suggesting the SDMBC surface is highly electronegative, it may be caused by the SDS is anionic surfactants and shield the positive charge on the SDMBC surface. In addition, SAP partially ionizes into negatively ions when the pH exceeds 4.6[42], this is also one of the reasons for the above-mentioned phenomenon.

Adsorption studies

Effect of pH

The pH of the solution a key factor affecting the absorption performance, as it affects not only the existing forms and the degree of ionization, but also affects the surface charge properties of adsorbent, as well as dissociative of functional groups on the active sites, and may cause an enormous change of the adsorbent removal efficiency[43], thus, it is necessary to investigate the influence of pH on sorption.

Results shown in Fig. 6, an increasing trend in MB removal efficiency was observed with the increasing pH value, suggesting that an alkaline conditions is more beneficial to MB adsorption, this reason is that the MB is a type of cationic dye. At lower pH value, there are a great number of H^+ in the solution, its might compete with MB for adsorption sites, and produce electrostatic repulsion, which is not conducive to MB adsorption. Indeed, at pH > 7, there are a great of OH^- in the solution, which lead to more anionic site on the surface of SDMBC, in return, enhances the electrostatic attractions between SDMBC and MB. Moreover, from Zeta analysis (Fig. 5),

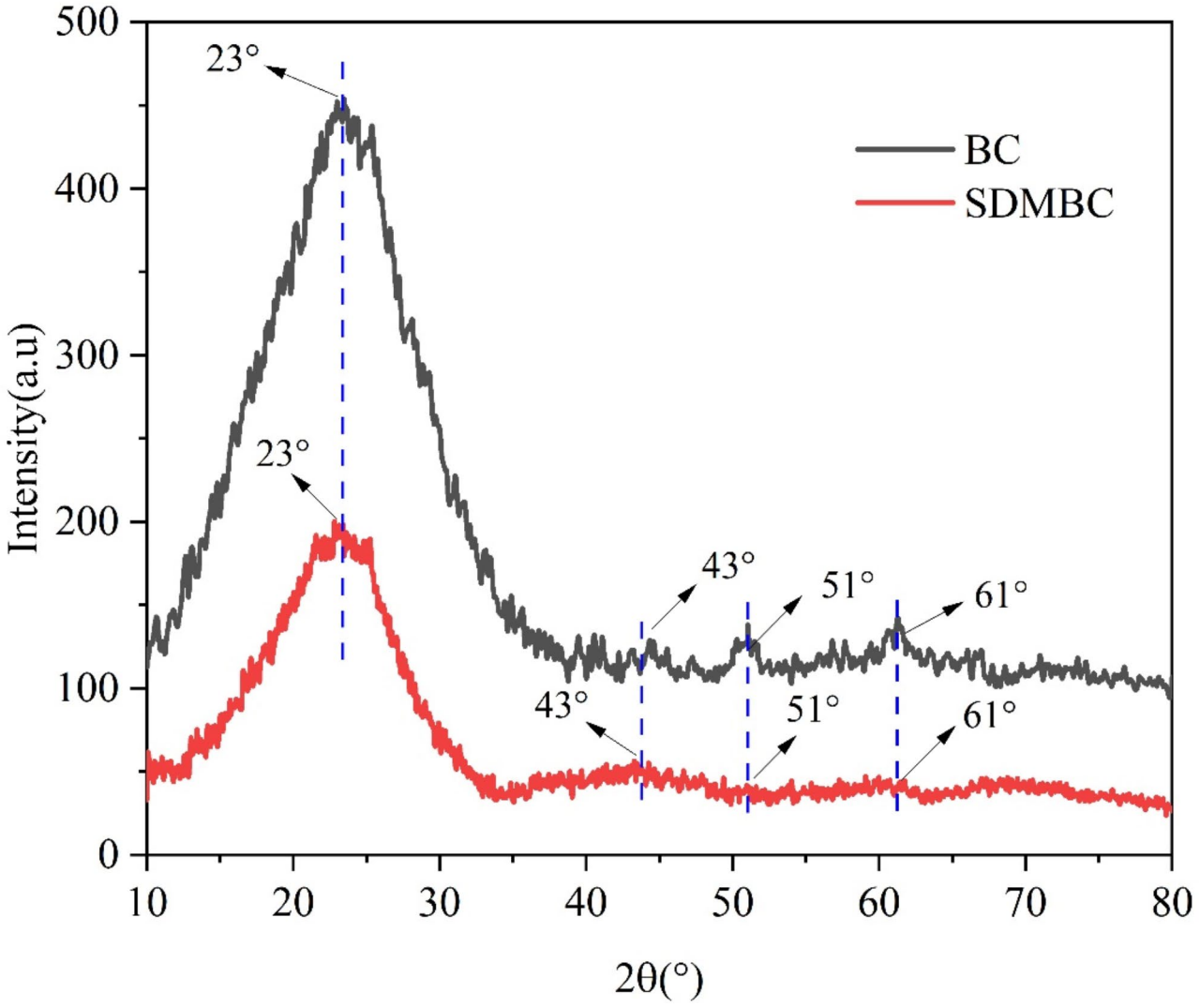

Fig. 3. XRD patterns of BC and SDMBC.

it can be know that the SDMBC provides a more negative charge with the rises of pH, making electrostatic interactions between MB and SDMBC was enhanced, thereby leading to an increased MB adsorption capacity. Finally, at the lower pH, acid exposure protonates the acidic functional groups on the SDMBC surface to produced $-OH^+$ and $-COOH_2^+$, these ions would cause electrostatic repulsion with MB, but, with increases pH value, H^+ concentration in solution decreasing, leading to protonation of oxygen-containing functional group decreasing[44], this not only enhanced the net negative charge on the SDMBC surface, but also enhanced MB interaction with the oxygen-containing functional group on the SDMBC surface, consequently the removal rate increase.

Effect of MB concentration on adsorption

Figure 7 illustrates the effect of different initial concentrations on MB removal ability. Firstly, with the increase of the MB concentration, the adsorption capacity of MB increase, can be attributed to the following reasons, on the one hand, the probability of collision between SDMBC and MB with an increase in the initial concentration of MB, which favors the adsorption of MB. On the other hand, the concentration difference between MB and SDMBC becomes larger when the MB initial concentration increases, this yields larger mass transfer forces are produced, which provides favorable circumstances for overcome the mass transfer resistance between the surface liquid phase and solid phase, thereby increasing adsorption amount[45]. On the contrary, with the increase of the initial concentration of MB, the removal efficiency shows a downward trend, this is since adsorption sites were abundant on the SDMBC surface when the MB concentration is low, can provide an enough number of adsorption sites for MB. Although the number of MB molecules keeps increasing, provides favorable conditions for adsorption, but, when the all adsorption sites were completely occupied by MB, the SDMBC cannot adsorb MB and eventually lead to cause reducing its removal efficiency.

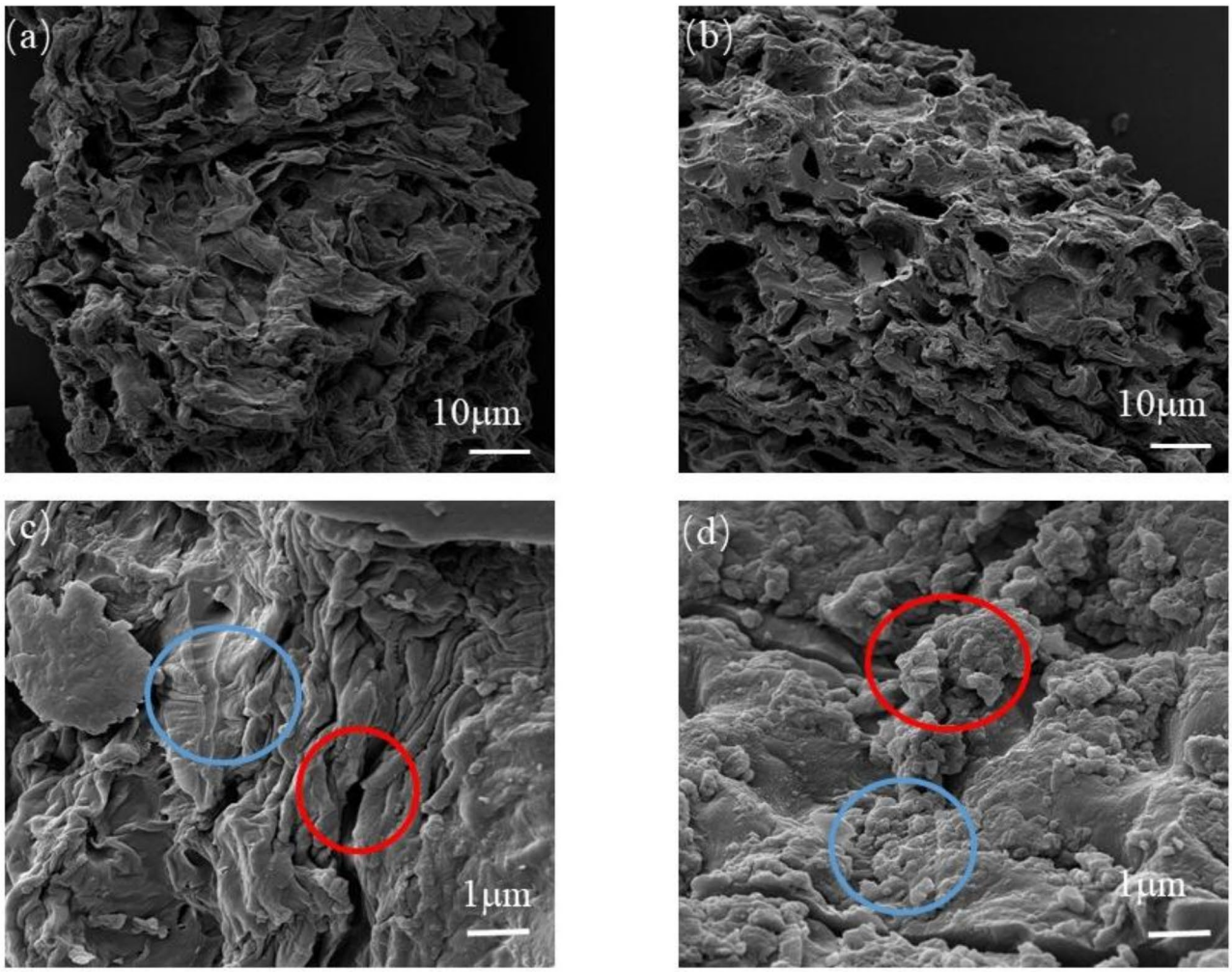

Fig. 4. SEM micrographs of BC (**a**,**c**) and SDMBC (**b**,**d**).

Effect of SDS/SAP ratio on adsorption

When the SDS/SAP composite system modifier concentration range from 0.2 CMC to 0.8 CMC, the MB rate increases with increasing concentration of modifier, and also reaches to best modification result at a concentration of 0.8 + 0.8 (Fig. 8). But, when exceeds 0.8 CMC, the removal rate of MB shows a decreasing trend. Without modification, BC poor dispersibility in water and poor binding affinity with MB, it is difficult to form an effective adsorption for MB. Once the BC were modified by a small amount of modifier, the dispersibility in water and affinity with MB of BC could be improved, and also as SAP/SDS concentration increased, more modifier molecules were adsorbed onto BC and spontaneously formed aggregates, which provides more adsorption sites for MB to gradually increase the adsorption performance. As the modifier concentration become close to the CMC, the formation of micellar aggregates on the surface of the BC, at this point, the adsorption capacity reached its maximum. But, with the increase modifier concentration, the BC pores were blocked by the modifier particles was increase, and thus, when the negative effect exceeded the positive effect of the modifying agent, which resulted the reduction in adsorption efficiency, this also explains why the removal rate of MB shows a decreasing trend at the SDS/SAP concentration above 0.8 + 0.8CMC.

Notably, after a series of modifications, the SDMBC exhibited a significantly higher adsorption capacity for MB, compared with BC, which mainly attributed due to the amount of active functional groups and adsorption sites was increased, and negative charge of SDMBC surface has been strengthened, lead to the SDMBC can provides more active sites, adsorb MB more favorably, this conclusion was also verified in FT-IR and XRD characterization. Finally, to better reflect the advantage of SAP/SDS composite system, under concentration of modifier is 0.8 CMC conditions, a series of control experiment were carried out (Fig. 8). As expected, SDS/SAP composite system had a better effect on increasing BC adsorption capacity, compared to single system, which can be explained by the following two aspects by the following two aspects, on the one hand, mixed surfactants are capable of lowering critical micelle concentration of surfactant, this facilitates the formation of micelles to provide favorable conditions for adsorption of MB[17]. On the one other hand, at pH value 7, SDS and SAP exists in the form of anions, providing ion-exchange sites for MB adsorption, thereby providing the great driving force for MB adsorption.

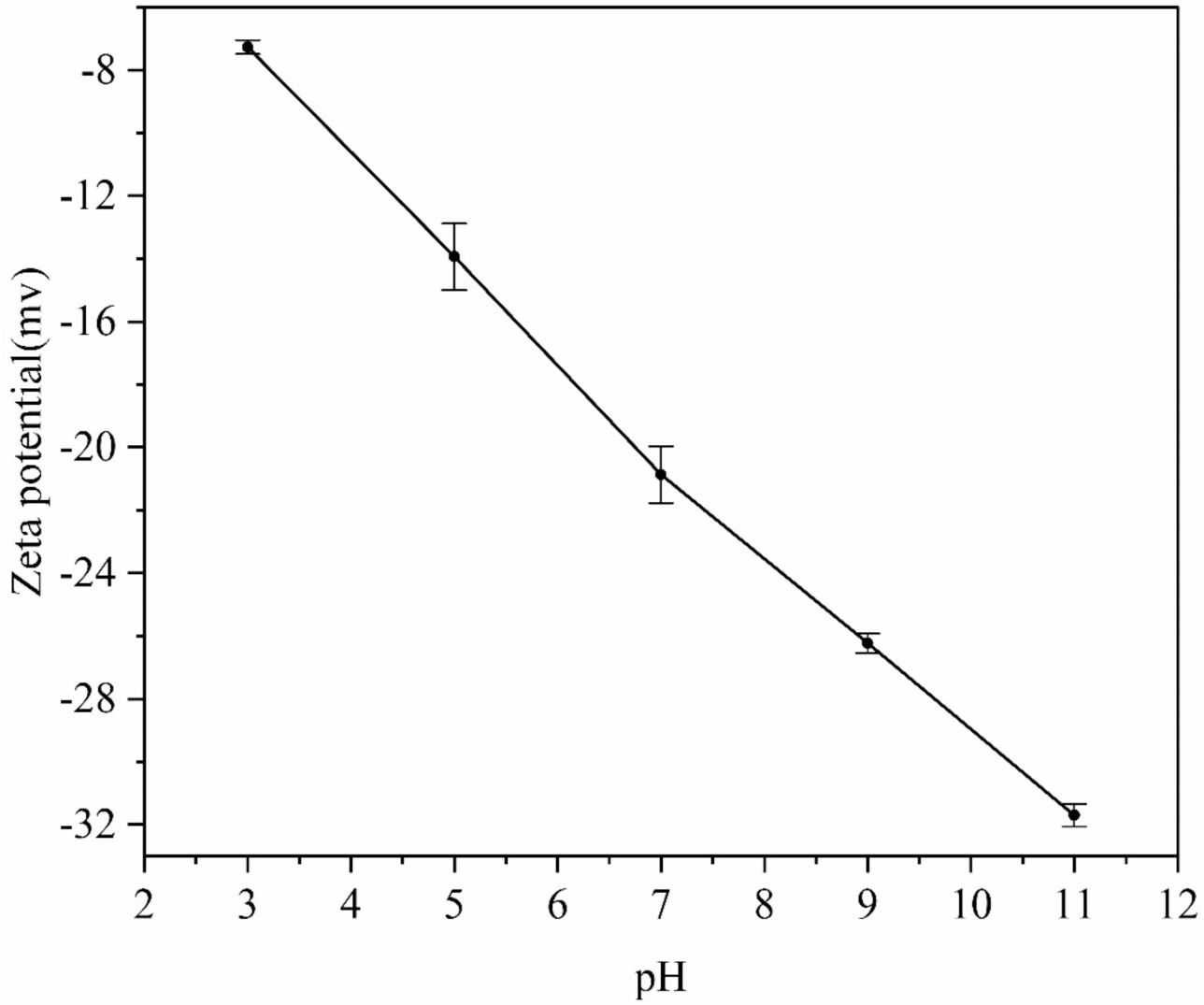

Fig. 5. Zeta potential of SDMBC at different pH.

Adsorption kinetic

Figure 9a–d shows the fitting results for the four kinetic model equations, respectively, the kinetic parameters show Table 1. The adsorption of MB on SDMBC followed pseudo-second-order kinetic model instead of pseudo-first-order kinetic model. Firstly, the calculated theoretical adsorption capacities by the pseudo-second-order kinetic model close with experimental data, while, the calculated theoretical adsorption capacities by the pseudo-first-order kinetic model have a big disparity to the experimental values. Secondly, the pseudo-second-order kinetic model correlation coefficient is greater than of the pseudo-first-order kinetic model correlation coefficient, indicating the MB adsorption by SDMBC is mainly a chemical adsorption.

But none them can be used describe the diffusion mechanism, therefor, the mechanism of diffusion was studied by intraparticle diffusion model. The results show that the intraparticle diffusion model not pass through the origin (Fig. 9c), denoting that intraparticle diffusion is not the only rate-restricting, and film diffusion mechanisms may also be involved[46], while, the C value with positive verified the correctness of the this speculation[47]. In addition, a large K_{dif} value may be related to the hydroxyl of MB forms a hydrogen bond with groups on SDMBC, and the increased carboxyl and hydroxyl groups on SDMBC6. Finally, the Elovich (Fig. 9d) also fits the experimental data with good accuracy ($R^2 = 904$), this result implies that during the MB adsorption process, the adsorption energy on the surface of the SDMBC are unevenly distributed, the active energy greatly changed during the adsorption process, and may occur chemisorption[48].

Isotherm studies

Figure 10a, b illustrates the fitting curves of the Langmuir and Freundlich model, respectively, and relevant fitting parameters are show in Table 2. The Frundlich isotherm model provided the better fit according to the correlating coefficient, which indicated that the SDMBC adsorption of the MB occurred mainly in double-layer adsorption, this is consistent with some previous studies on biochar-mediated MB adsorption[47].

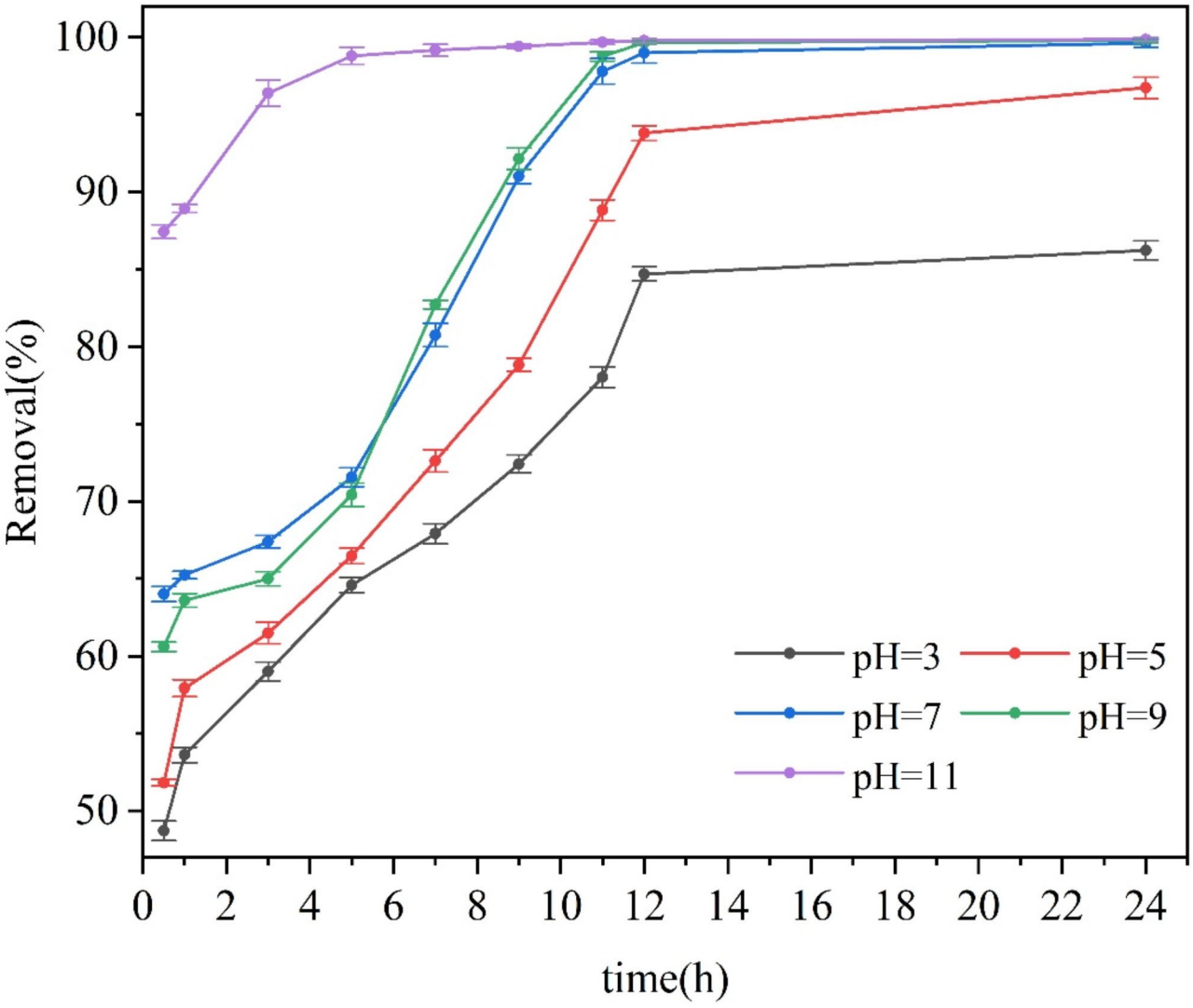

Fig. 6. Effect of pH on adsorption of MB (at pH = 11, the maximum removal efficiency of 99.5%).

The intensity parameter (1/n) of Freundlich and the separation factor (R_L) of Langmuir were in the range of 0 to 1, which revealed that the adsorption process is favorable[49], and also further confirm that the SDMBC is an effective sorbent for remove MB from solution. Besides, the MB adsorption ability of SDMBC maximizes to 277.086 mg/g at 308 K, the K_L value q_m increases with increasing temperature, suggesting that the increasing the temperature was conducive to adsorption. The Freundlich constant k_F increased from 104.250 to 155.896 with the increase of temperature, which indicates that the interaction between MB and SDMBC increases with increasing temperature. Moreover, the 1/n and R_L value decrease with increasing temperature also suggesting the intensity of the adsorption inducement enhanced when the temperature was increased[50]. Similar results was reported in an MB removal study by Wang et al.[51].

In this study article, the MB adsorption capacity of SDMBC was also compared with other materials. It can be seen from Table 3 that adsorption capacity of SDMBC for MB above most previously reported adsorbents, showing superiority of SDMBC. Additionally, taking into account of modification method simple, effective and sustainable, what more important, the proposed method increased the adsorption capacity and the number of functional groups of BC significantly, indicating that this method is also applicable to improve the capacity ability of other adsorbents, this reflects the general applicability of the method.

Effect of coexisting pollutants on the adsorption

In order to explore the potential of the SDMBC application as a sorbents in sewage purification, OP with difference properties and HMs were selected as object pollutants, including BPA (is a hydrophobic OP, at pH = 7, it exists mainly in neutral molecular form), PNP, (at pH = 7, it exists in the anionic form), MB (is a water-soluble cationic dye), Cd(II) and pb(II), the adsorption capabilities of SDMBC for each pollutants was examined in single, respectively. For details, please see supplementary materials 3 (Sect. 2.4.7).

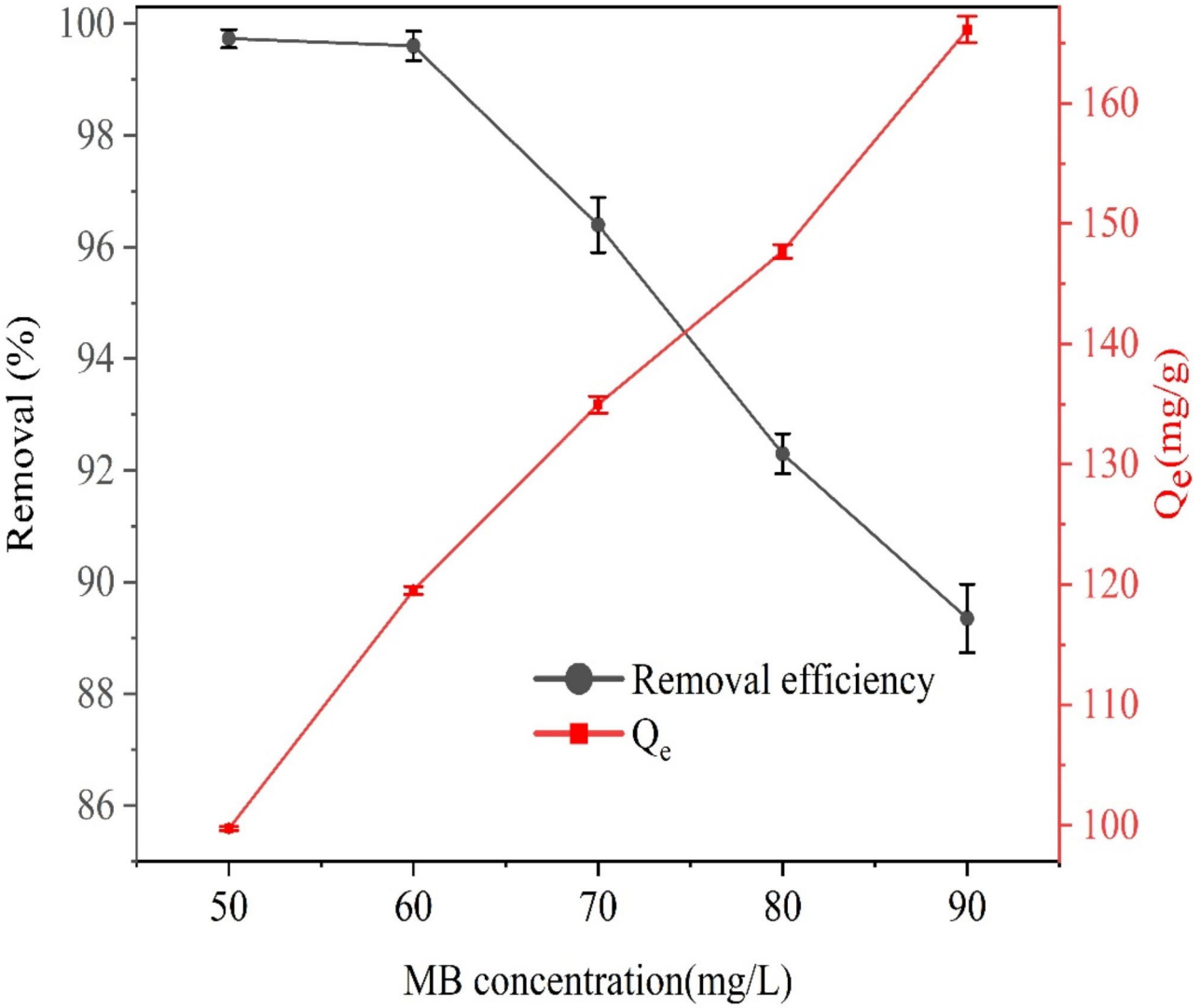

Fig. 7. Effect of concentration on adsorption for MB (The equilibrium adsorption amount was 166.12 mg/g, at $C_0 = 90$ mg/L).

As shown in Fig. 11, SDMBC exhibits excellent removal performance, the adsorption capacity of pb(II), Cd(II), MB, PNP and BPA were 130.23, 108.43, 134.95, 112.78, 125.27 mg/g, respectively, better than most reported adsorbents (see Table 3). The formation of complexation and electrostatic force between SDMBC with HMs, as well as interactions between OP and SDMBC including hydrogen bond, π-π interaction, hydrophobic interactions, electrostatic attraction is main reason for highly efficient adsorption. Moreover, the SAP/SDS nanomicelle were crosslinked onto surface of SDMBC, this can provides abundant active sites for adsorption, giving SDMBC excellent removal properties. SDMBC showed the best adsorption performance for MB, therefore, we chosen MB as representative to build machine learning prediction models and competitive adsorption analysis.

Adsorption study in a binary process

The removal performance of SDMBC toward individual pb(II), Cd(II), BPA, PNP and MB pollutant in binary systems (PNP, Pb(II), Cd(II), BPA-MB) was conducted and compared with the mono system. For details, please see supplementary materials 3 (Sect. 2.4.7).

Competitive adsorption of PNP and MB analyze

The PNP molecule possess hydroxyl groups and aromatic rings, both can form hydrogen bonds with the hydroxyls and carboxyls of SDMBC, the electrostatic force between nitro group (electron-withdrawing group) and phenolic hydroxyl (electron-donating group) of PNP molecule promote the formation of π-electron cloud, as well as the aromatic ring of PNP provide π electronic, formed π-π interaction with the π-electron-donor functional groups of SDMBC, such as C = C, -OH and –COOH[63]. Moreover, SDMBC has a hydrophobic cavity, PNP could be fix into the hydrophobic core by hydrophobic force[64], which provides the strong impetus for PNP

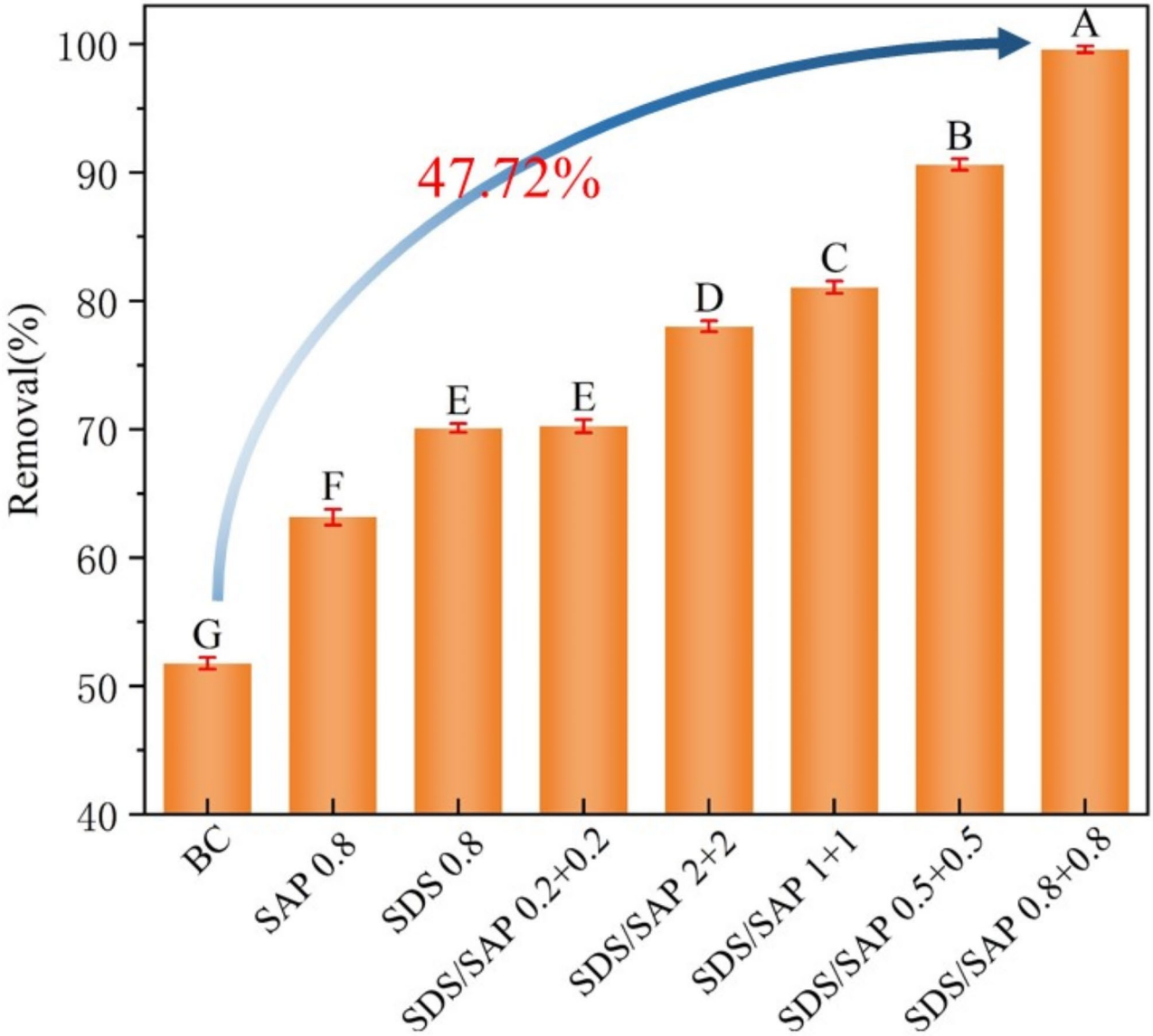

Fig. 8. Impact of different SAP/SDS Ratios on adsorption. (The best SDS/SAP concentration is 08 + 0.8CMC). Note: Different capital letters indicate significant differences within groups (P<0.01).

removal (Fig. 12A). thus, SDMBC exhibits excellent adsorption performance for PNP. In addition, the hydrogen bonding, π-π interaction and electrostatic attraction is the primary mechanism of the SDMBC removal of MB (see Fig. 17 for details).

What is more interesting, the removal efficiency of PNP by SDMBC in the binary system increased slightly, increased from 112.78 to 128.53 mg/g (Fig. 12B), this can be attributed to the electrostatic shielding effect of MB, which can cause the reduction in electrostatic repulsion between SDMBC and PNP. While, competition for active site between PNP and MB is the main reason for MB removal ability decreased (134.95 mg/g to 124.86 mg/g). Importantly, the main driving force of PNP and MB adsorption onto SDMBC were big different (electrostatic attraction and hydrogen bonding for MB, hydrogen bonding, hydrophobic interaction and π-π interaction for PNP), thus, can effectively avoid competition, ultimately maintains efficient removal capability.

Competitive adsorption of BPA and MB analyze

As shown in Fig. 13A, the aromatic ring structure of SDMBC is conducive to the formation of hydrogen bonds with BAP having benzene ring. The hydrophobic interactions between BPA and SDS/SAP. The BPA possess hydroxyl could easily form hydrogen bonds with hydroxyl of SAP. Micelle structure of SAP/SDS with hydrophobic core, which can direct encapsulate BPA in its core to form stable inclusion complex, this provide strong driving for BPA removal[65].

The binary competitive adsorption has a little effect on the removal ability of MB and BPA, the adsorption capacity of SDMBC to BPA and MB decreased from 125.27, 134.95 to 110.40, 119.81 mg/g, reduction of 11.87%

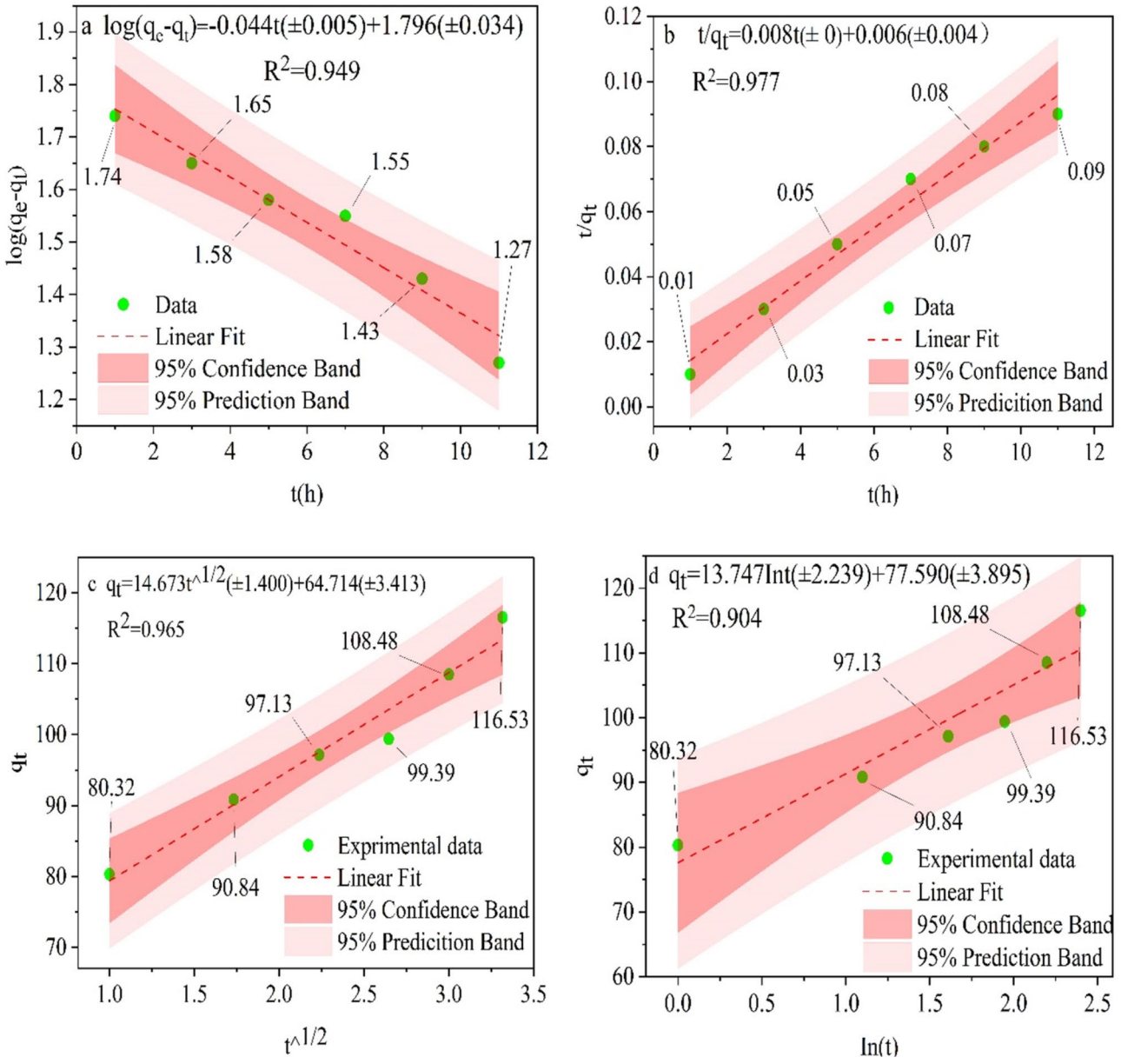

Fig. 9. (**a**) pseudo-first-order kinetic model, (**b**) pseudo-second-order kinetic model, (**c**) intraparticle diffusion kinetic model, and (**d**) Elovich model, (Pseudo second order model fits experimental data best).

and 11.23%, respectively (Fig. 13B).The adsorption of BPA onto SDMBC mainly through and π-π interaction[66], while MB is mainly attributed hydrogen bonding and electrostatic attraction. Moreover, relevant studies indicate that BPA removal may be viewed as a partitioning process of BPA to the micellar core instead of adsorption[67], in the presence of surfactants, thus, the competitive adsorption between BPA and MB is very weak. A similar result has been gived from recent simultaneous removal of MB and BPA experiments performed by Hemine et al.[68].

Competitive adsorption of pb(II) and MB analyze

As shown in Fig. 14A, for pb(II) removal, the some ionizable function groups, such as carboxyl groups (COOH) of SAP and sulfonate (SO^{3-}) groups of SDS, which could interact with pb(II) via electrostatic attraction, the protons H^+ of acidic functional groups and Na^+ of SDS can be ion-exchange with pb(II), moreover, complexation between carboxyl groups and hydroxyl groups with pb(II) played an important role for pb(II) adsorption on SDMBC[23].

In the binary system, the adsorption capacity of SDMBC to pb(II) and MB decreased from 130.24, 134.95 to 102.62, 114.65 mg/g, respectively (Fig. 14B), due to MB compete with pb(II) (for active groups such as carboxyl groups, hydroxyl groups) and overlap among the adsorption mechanism[69]. But, SDMBC still maintains efficient removal performance for MB and pb(II), this can be attributed to SAP with extremely strong complexing ability for pb(II), comparable to inorganic acid and even higher than chelating agent[25], thus, the competition for

	Parameters	The value of parameters
Kinetic model	qe cal (mg/g)	62.572
	qe exp (mg/g)	116.527
Pseudo-first-order	k_1 (h^{-1})	0.099
	R^2	0.949
	q_e cal (mg/g)	122.850
	q_e exp (mg/g)	116.527
Pseudo-second-order	K_2 (g/mg min^{-1})	1.182
	R^2	0.977
	K_{dif} (mg/g $min^{-1/2}$)	64.714
Intraparticle diffusion	C	14.673
	R^2	0.965
	α (mg/g min^{-1})	13.747
Elovich	β mg/g	73.590
	R^2	0.904

Table 1. Kinetic parameters for the adsorption of MB onto SDMBC (Pseudo second order model fits experimental data best).

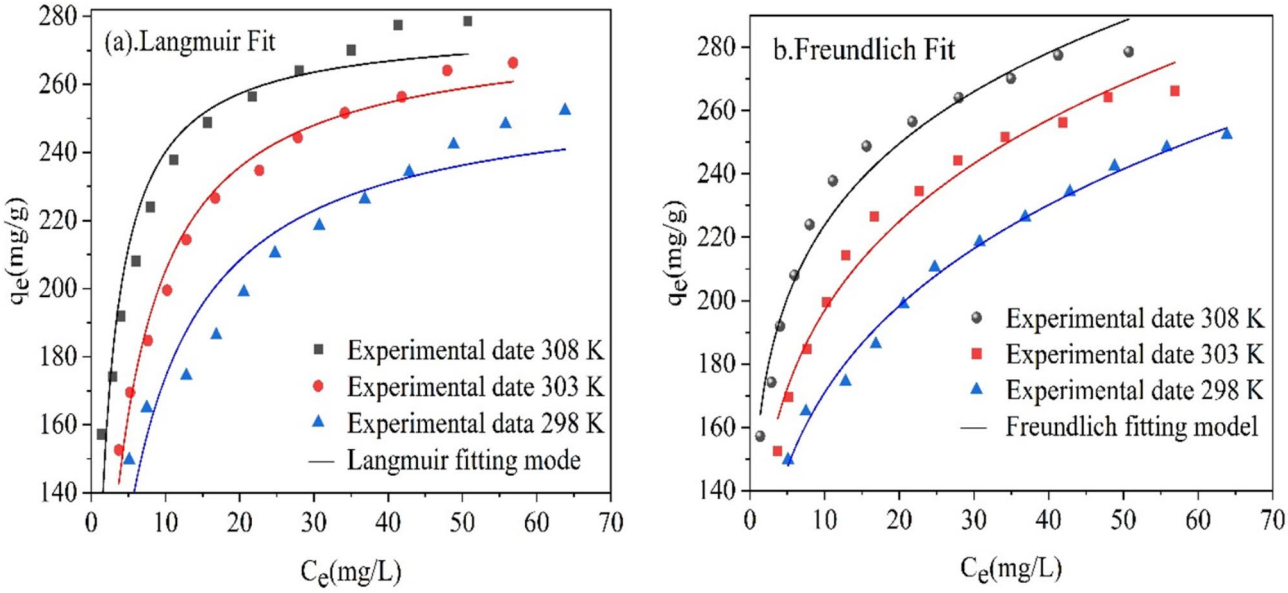

Fig. 10. Adsorption isotherms for MB adsorption on SDMBC modeled with (**a**) Freundlich and (**b**) Langmuir, (Langmuir isotherms gives maximum capacity 277.09 mg/g, and Freundlich model provided better fit).

Isotherm model	Parameters	Parameter value		
		298 K	303 K	308 K
	K_L(L/mg)	0.203	0.286	0.649
Langmuir	q_m(mg/g)	259.441	276.844	277.086
	R_L	0.025–0.059	0.018–0.041	0.008–0.019
	R^2	0.906	0.982	0.932
	K_F	104.250	126.346	155.896
Freundlich	1/n	0.214	0.193	0.157
	R^2	0.991	0.972	0.969

Table 2. Parameters of isotherms and and correlation coefficients for MB adsorption on SDMBC (Freundlich model provided better fit).

Number	Adsorbent	Adsorbates	q_m(mg/g)	Refs.
1	Sludge-derived granular biochar	BPA	84.78	[52]
2	CDP@Fe_3O_4	BPA	115.47	[3]
3	UFA-DB -SA tri-composite beads	BPA	16.6	[53]
4	TMPTA-CE	PNP	98.03	[54]
5	Biochar form Pine sawdust	PNP	117.17	[55]
6	Alfalfa biochar	PNP	49.25	[56]
7	nitrogen doped magnetic carbon aerogel	pb(II)	65	[4]
8	H_3PO_4 – modified tea branch biochar	pb(II)	127.5	[57]
9	PASP-BC	pb(II)	126.1	[58]
10	BCHMn	Cd(II)	108.21	[59]
11	biochar properties	Cd(II)	66.68	[38]
12	H_3PO_4 – modified tea branch biochar	Cd(II)	98.25	[57]
13	PAN-H/β-CD	MB	216.94	[60]
14	WQM1	MB	244.6	[61]
15	BMNC	MB	128	[62]
16	SDMBC	MB, BPA, PNP	276.08, 125.27, 112.78	This study
		Pb(II), Cd(II)	130.23, 108.43	

Table 3. Compared with other adsorbents.

available adsorption site between pb(II) and MB were greatly weakened, ensures MB and pb(II) to have its own adsorbing site.

Competitive adsorption of Cd(II) and MB analyze

Similarly, as observed from Fig. 15A, the electrostatic attraction between SDMBC and Cd(II), complexation of oxygen functional groups (hydroxyl and carboxyl groups) with Cd(II)[70], the graphene-like structure and aromatic carbon of SDMBC has rich π-electron system that ability forming cation–π interaction with cd(II) due to electron deficiency[71]. as well as ion exchange between Na^+ in the SDS molecules, protons H + of acidic functional groups and Cd(II)[72], these provides basis for efficient Cd(II) removal. Both coexist did not influence the uptake of MB and Cd(II) obviously, Cd(II) and MB decreased from 108.43, 134.95 to 94.38, 116.30 mg/g, reduction of 12.96% and 13.82%, respectively (Fig. 15B), a reasonable explanation might be that the double layer of MB on SDMBC, which provide additional cationic point for Cd(II)67.

Adsorption thermodynamics

According to the effect of different temperatures on the adsorption capacity, the thermodynamic parameters (ΔG, ΔH and ΔS) were evaluated and summarized parameters are list in Table 4. The negative ΔG values explained that the adsorption of MB on SDMBC is a spontaneous process. The absolute values of ΔG increases with increasing temperature, suggesting that adsorption was conducive by increasing temperature, the positive ΔH indicated that adsorption process was endothermic. Additionally, the obtained negative ΔS value, which showed that process were mainly driven by enthalpy[73]. Similar results were obtained from other researchers, such as MB adsorption onto porous organic polymer[74].

Sorption mechanisms

In order to further explore the adsorption mechanism of MB on SDMBC, the FT-IR of adsorption MB before and after were analyzed and compared, and combined effect of pH value, co-existing ion and Zeta analysis proposed a possible adsorption mechanism.

As show in Fig. 16, the peaks characteristic for MB appear in SDMBC, such as symmetric stretching of C-N (1382 cm^{-1}) and stretch vibrations of methyl symmetric (1328 cm^{-1}) deformation after adsorption MB, suggesting that MB was successfully adsorbed on SDMBC[74]. Methyl symmetric deformation of in MB migrated from 1341 cm^{-1} to 1328 cm^{-1}, symmetric stretching of C-N in MB migrated from 1397 cm^{-1} to 1382 cm^{-1}, and vibration C = O of carboxyl on SDMBC migrated from 1573 cm^{-1} to 1582 cm^{-1} after adsorption MB, indicating that electrostatic interaction between $-N(CH_3)_2^+$ in MB and negatively-charged carboxylate in SDMBC[75,76]. Furthermore, combines effect of initial pH value and coexisting cations (see Fig. 181 for details) on adsorption capacity of MB also manifest that electrostatic attraction has played an important role in adsorption process of MB by SDMBC[63]. Vibration C-H of aromatic in MB migrated from 886 cm^{-1} to 876 cm^{-1}, vibration C-H of aromatic on a SDMBC from 870 cm^{-1} shifts towards higher and the peak becomes sharper, after adsorption MB, which suggest that presence of weak π-π interaction between MB and SDMBC[36]. Finally, the peak at 3400 cm^{-1} weakens and eventually disappears, this means that existence of weak hydrogen bond interaction between SDMBC and MB[77]. Summary, the possible mechanism of adsorption toward MB by the SDMBC includes electrostatic attraction, hydrogen bonding and π–π interaction. The detailed mechanism of SDMBC for MB are shown Fig. 17.

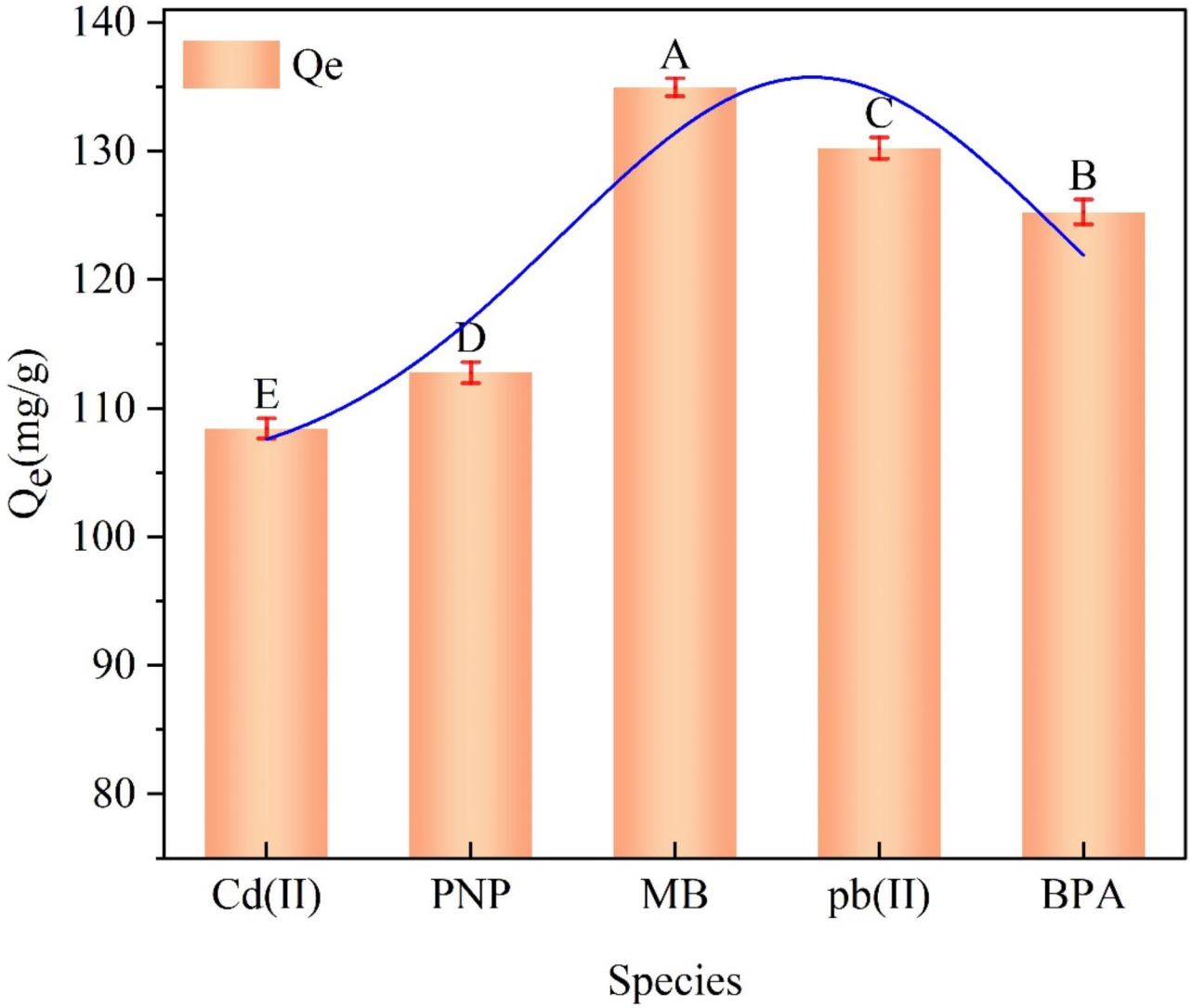

Fig. 11. The adsorption performance of SDMBC for different pollutants. Notes: different capital letters indicates significant differences within groups ($P<0.01$). (For Cd (II), PNP, MB, pb(II), and BPA adsorption capacities 108.43, 112.87, 134.96, 130.24 and 125.27 mg/g, respectively).

Effect of ionic strength

Generally speaking, there are many kinds inorganic salt ions in actual water (such as Na^+, Ca^{2+} and HCO_3^-), on the one hand, them may compete with target pollutant for adsorption site, on the other hand, also possibly affect the hydrophobicity and solubility of target pollutant, which affects the removal of pollutant. For details, please see supplementary materials 3 (Sect. 2.4.8).

As shown in Fig. 18, the adsorption capacity of SDMBC for MB show deceased of trend in the present of cation (Na^+ and Ca^{2+}), this can be attributed to the competition between co-existing cation (Na^+, Ca^{2+}) and MB for the adsorption sites, this result also show that the electrostatic interaction is one of the main mechanisms of the adsorption of MB by SDMBC[78], similar results was reported in the MB adsorption by peanut hull study[79]. Obviously, effect of Ca^{2+} on adsorption for MB was greater than Na^+, which might be interpreted to following two reason, on the one hand, the higher valence ions can easily adsorb to the adsorbent surface and weakens the charge of adsorbent surface, this makes them more aggregate, on the other hand, Na^+ can occupy only one ion-exchange site in a SDMBC, while Ca^{2+} can occupy two ion interaction site.

While, the presence of anion (HCO_3^-) can promote the MB adsorption on SDMBC, this can be interpreted as the HCO_3^- covered on the adsorbent surface, which can provide more negative ions adsorption sites for MB molecules by "bridging" mode. But it is noteworthy that SMBC still had the efficient removal ability (above 70% of the original adsorption capacity even in the presence of competing ions at high concentrations (0.1 mol/L)), suggesting competing ions had little impact on MB removal of SDMBC, which provides possibility for practical application of SDMBC.

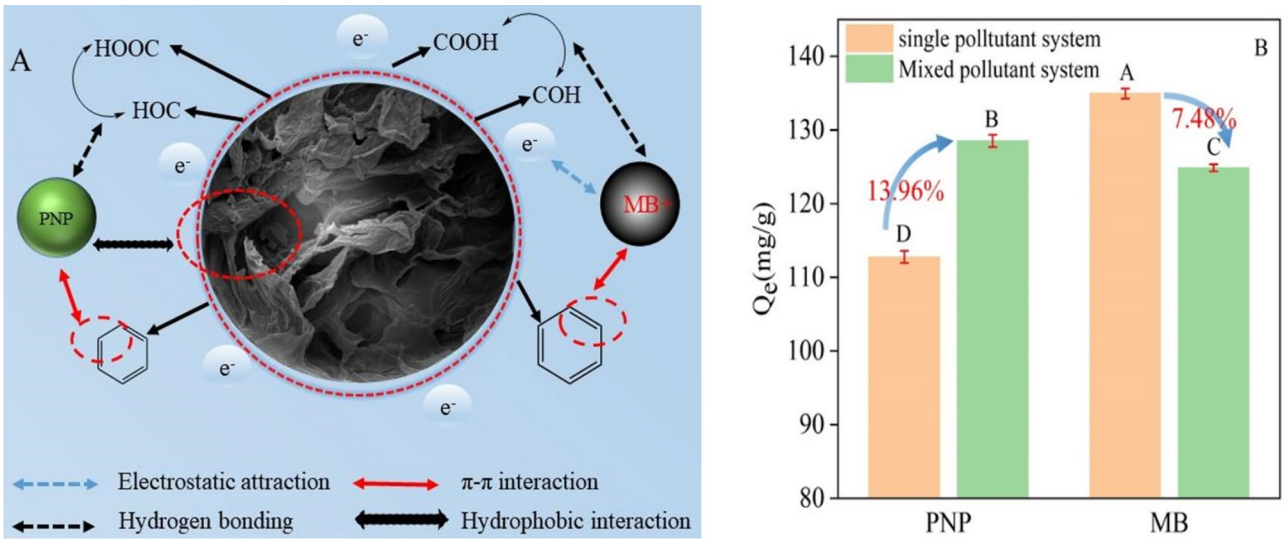

Fig. 12. Schematic diagram of the MB and PNP adsorption on SDMBC. Notes: Different capital letters indicates significant differences within groups (P<0.01).

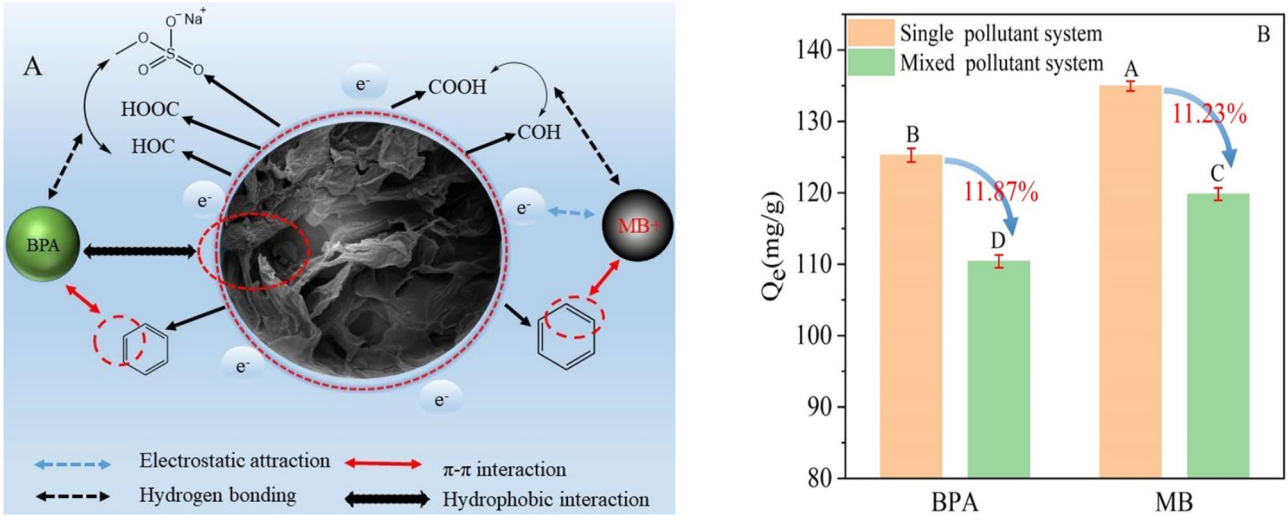

Fig. 13. Diagram of the removal process for MB and BPA by SDMBC. Notes: Different capital letters indicates significant differences within groups (P<0.01).

Reusability of SDMBC

The reusability of the SDMBC were investigated by adsorption-desorption. For details, please see supplementary material 3 (Sect. 2.4.9). As show in Fig. 19, the SDMBC still keep high and steady removal rates even after 5 reuses, indicating excellent regeneration properties of the SDMBC and is a promising material for MB removal.

Cost analysis

Obtaining feedstock at low or no cost is very important, and SPF, a by-product of *Sapindus* indica processing, fulfils this very well as it is available at no/very low cost and can provide a sustainable supply for BC production. To calculate the production cost of SDMBC the cost of chemicals and energy consumed during this preparation has been kept in mind. Here, to prepare 1 kg of SDMBC the cost was calculated using following equations: (5) to (8)[80].

$$\eta(\%) = \frac{\boldsymbol{X}}{\boldsymbol{Y}} \times 100\% \tag{5}$$

Where, X and Y indicates the SDMBC and SPF, respectively; η indicates BC harvest rate.

$$\text{Chemical cost } (\$) = \text{Chemical required } (\text{kg or L}) \times \text{Unit cost of chemical } (\text{kg or L}/\$) \tag{6}$$

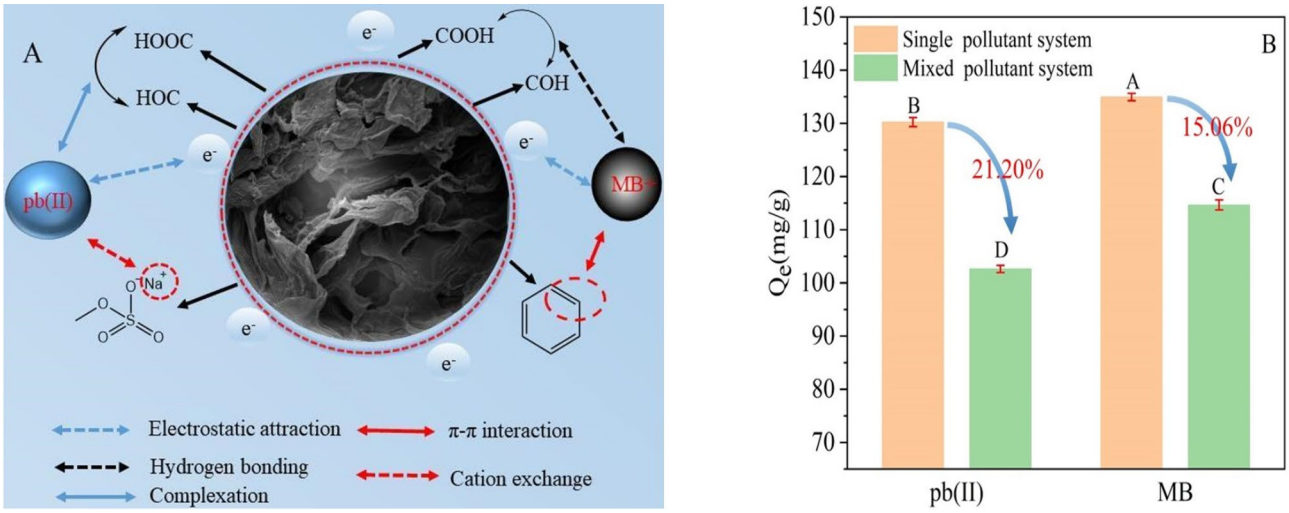

Fig. 14. Proposed possible mechanism of pb(II) and MB adsorption on SDMBC. Notes: Different capital letters indicates significant differences within groups (P<0.01).

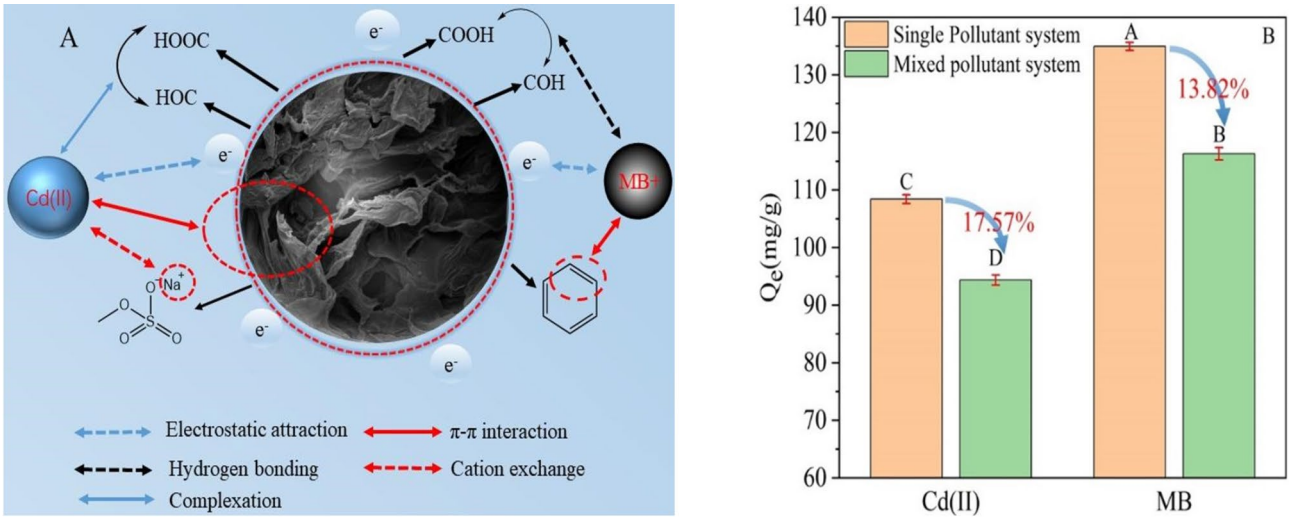

Fig. 15. Proposed mechanisms of Cd(II) and MB onto SDMBC during adsorption process. Notes: Different capital letters indicates significant differences within groups (P<0.01).

T	ΔG	ΔH	ΔS	R^2
(K)	K J/mol	K J/mol	J/mol K	
298	-10.001			
303	-11.697	14.99	54.275	0.975
308	-14.533			

Table 4. Thermodynamic parameters for MB adsorption onto SDMBC.

$$\text{Power consumed } (KW.h) = \text{Power (W)} \times \text{Time (S)} \quad (7)$$

$$\text{Energy cost (\$)} = \text{Power consumed } (KW.h) \times \text{Electricity cost } (KW.h/\$) \quad (8)$$

$$\text{Total cost (\$)} = \text{Eq. (19)} + \text{Eq. (21)}$$

Where, the cost of chemical reagents (SDS, SAP, HNO_3) were taken from latest supplier pricelist (Table 5). Considering that SPF is a processing residue, its price is very low and therefore, the SPF price is negligible. As it can be seen from Table 5, the total preparation cost of 1 kg SDMBC has been found in order of 46.45$, the cost

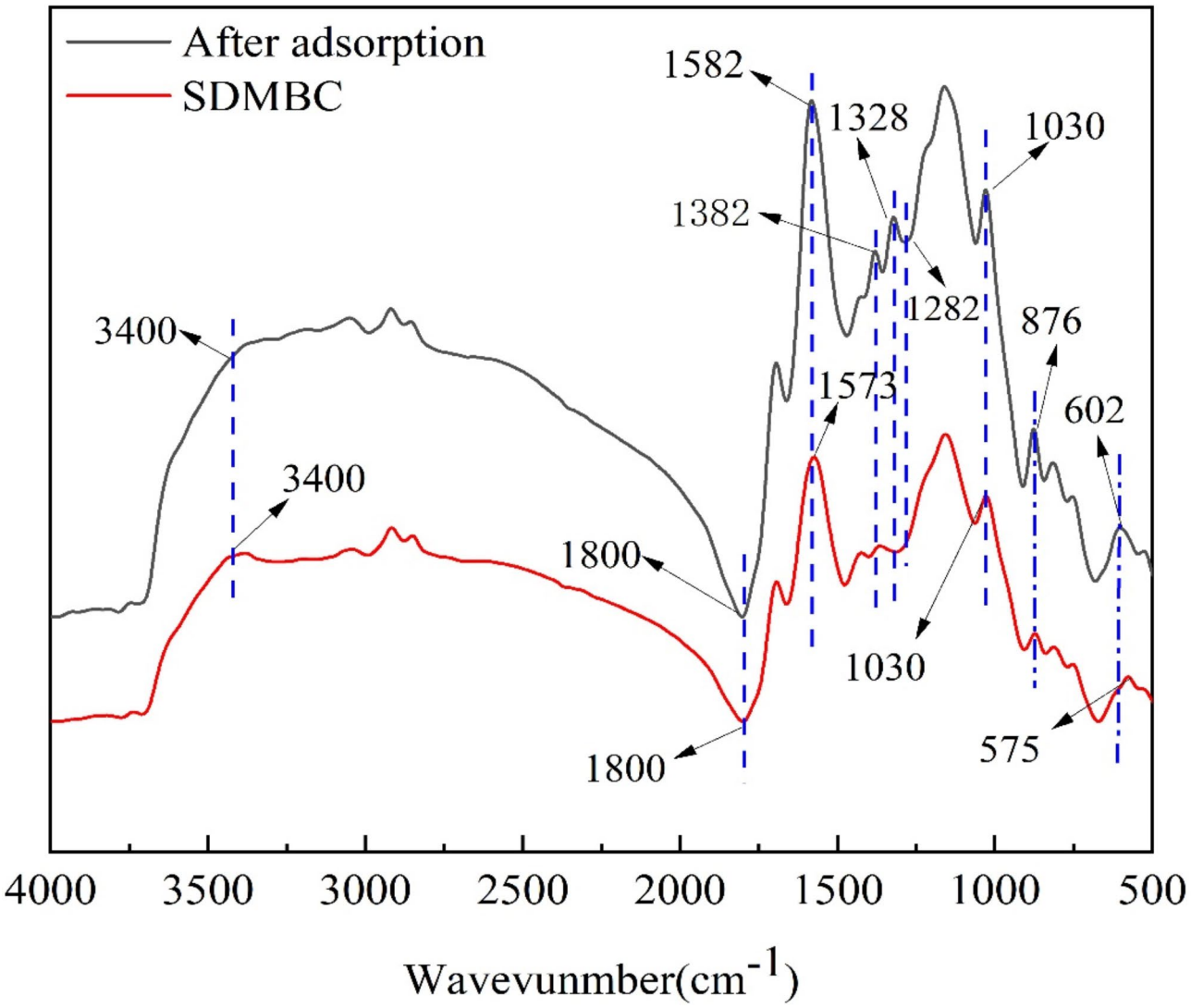

Fig. 16. FT-IR spectra of SDMBC before and after MB adsorption.

of SDMBC much lower compared with other adsorbent (Table 6). However, the cost is a little bit high because preparing on a lab-scale, but when it will be prepared on a large scale for commercial use its cost will cut down to a great extent.

Adsorption isotherms are an important tools for designing adsorption systems and predicting the mass of SDMBC, m (g), required to remove MB from a volume V (L) effluent, from a known initial amount (Co (mg/L)), to a preset concentration((Ce (mg/L). This is of great significance for in the evaluation economic benefits of adsorbents. Sips model fitting cannot be well experimental data (Table 7), therefore, it was decided to exclude Spis in our work. Since the equilibrium data were best fitted by the Freundlich Isotherm, thus, we implement the following equations make predictions[81,82].

The adsorption capacity (q_e, mg/g) and rate (R, %) of MB on adsorbent were calculated by Eq. (9) and Eq. (10), respectively:

$$q_e = \frac{(C_0\text{-}C_e)V}{m} \tag{9}$$

$$R = \frac{C_0\text{-}C_e}{C_0} \times 100\% \tag{10}$$

The Freundlich equation is represented as:

$$q_e = K_L C_e^{\frac{1}{n}} \tag{11}$$

Equating Eqs. (5) and (11) and rearranging, gave Eq. (12):

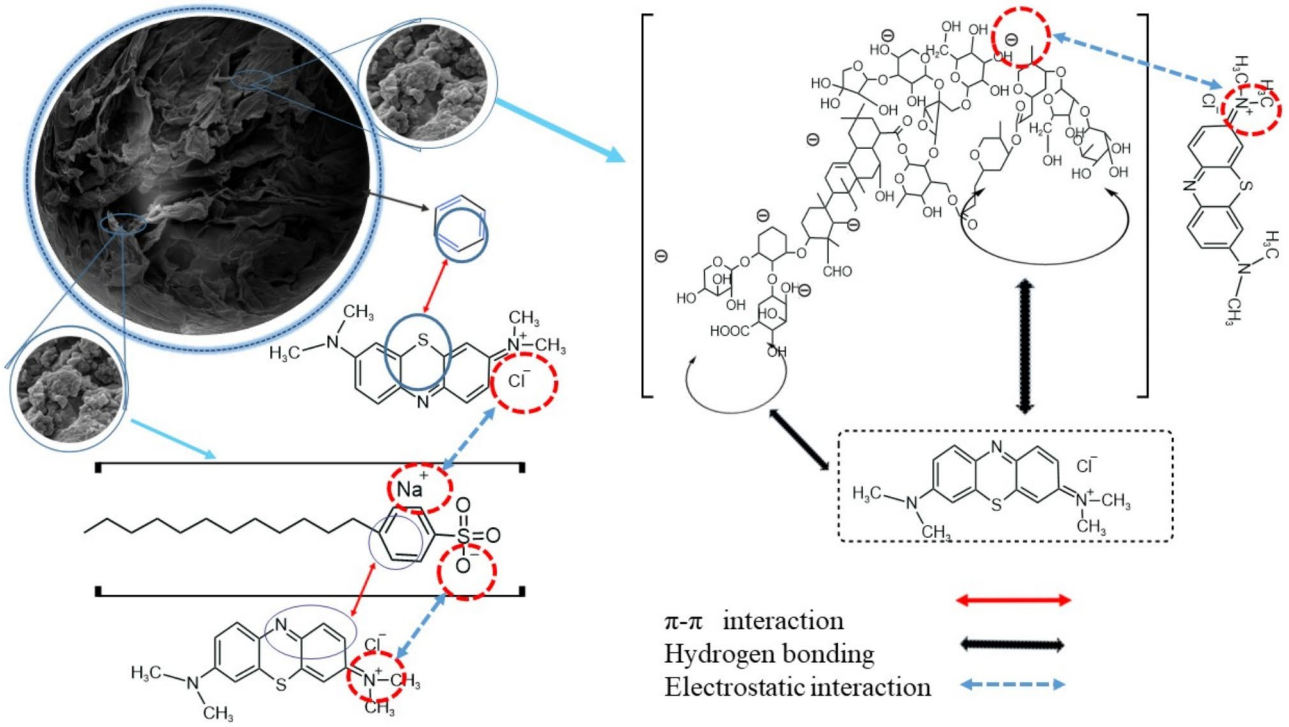

Fig. 17. The possible mechanism of adsorption toward MB by SMBC. (Adsorption mechanism includes hydrogen bonding, π-π interaction, electrostatic interaction).

$$m(g):=\frac{(C_0\text{-}C_e)\,V}{K_F C_e^{\,1/n}} \tag{12}$$

Rearranging Eq. (6) gives rise to Eqs. (13) and (14):

$$C_0\text{-}C_e=\frac{RC_0}{100} \tag{13}$$

$$C_e=C_0\left(1\text{-}\frac{R}{100}\right) \tag{14}$$

Replacing Eqs. (13) and (14) into Eq. (12) we obtained Eq. (15):

$$m(g)=\frac{RC_0V}{100K_F\left[C_0\left(1\text{-}\frac{R}{100}\right)\right]^{1/n}} \tag{15}$$

Where, Co is the initial concentration of MB (mg/L), Ce stands for the MB concentration at equilibrium (mg/L), V is the volume of solution (L); m: mass of absorbent (g), R is the percentage removal (%), K_F and 1/n is the values of the Freundlich isotherm constants (308 K).

Figure 20 shows the predicted the mass of SDMBC required for 99% sequestration of MB from effluents of different volumes. An initial concentration of 60 mg/L was used. From the fitting diagram, a dose of 4.13 g of SDMBC is required to Remove 99% of 60 mg/L MB from a 10 L effluent provides evidence that SDMBC is a cheap efficient adsorbent.

ML performance evaluation

In this work, seven ML models (BP, CNN, SVR, PF, LsBoost, AbaBoost, XGBoost) were applied to predict of MB removal by SDMBC. As can be seen from Table 8, the R^2 value training and test of the BP, CNN, SVR, PF, LsBoost, AbaBoost and XGBoost are 0.967, 0.979, 0.963, 0.834, 0.991, 0.894 and 0.998; 0.924, 0.937, 0.706, 0.784, 0.915, 0.764 and 0.976, respectively. Figure 21 exhibiting regression plots between output value and predicted value of all models, among them, the XGBoost also demonstrated best performance. More, XGBoost has the lowest MAE and RMSE (In the training phase, MAE, RMSE value 0.547, 0.831, during the test phase, MAE and RMSE value 2.680, 3.433, respectively), suggesting the XGBoost is the best model in this study, this result can be attributed to the decision tree in XGBoost model can be corrected iteratively[83], this is to say, the first decision tree, if cannot fix errors very well, next, build second decision tree based on the prediction results of previous tree, to further fix incorrect predictions, repeating this process, each new tree trying to correct for the all errors

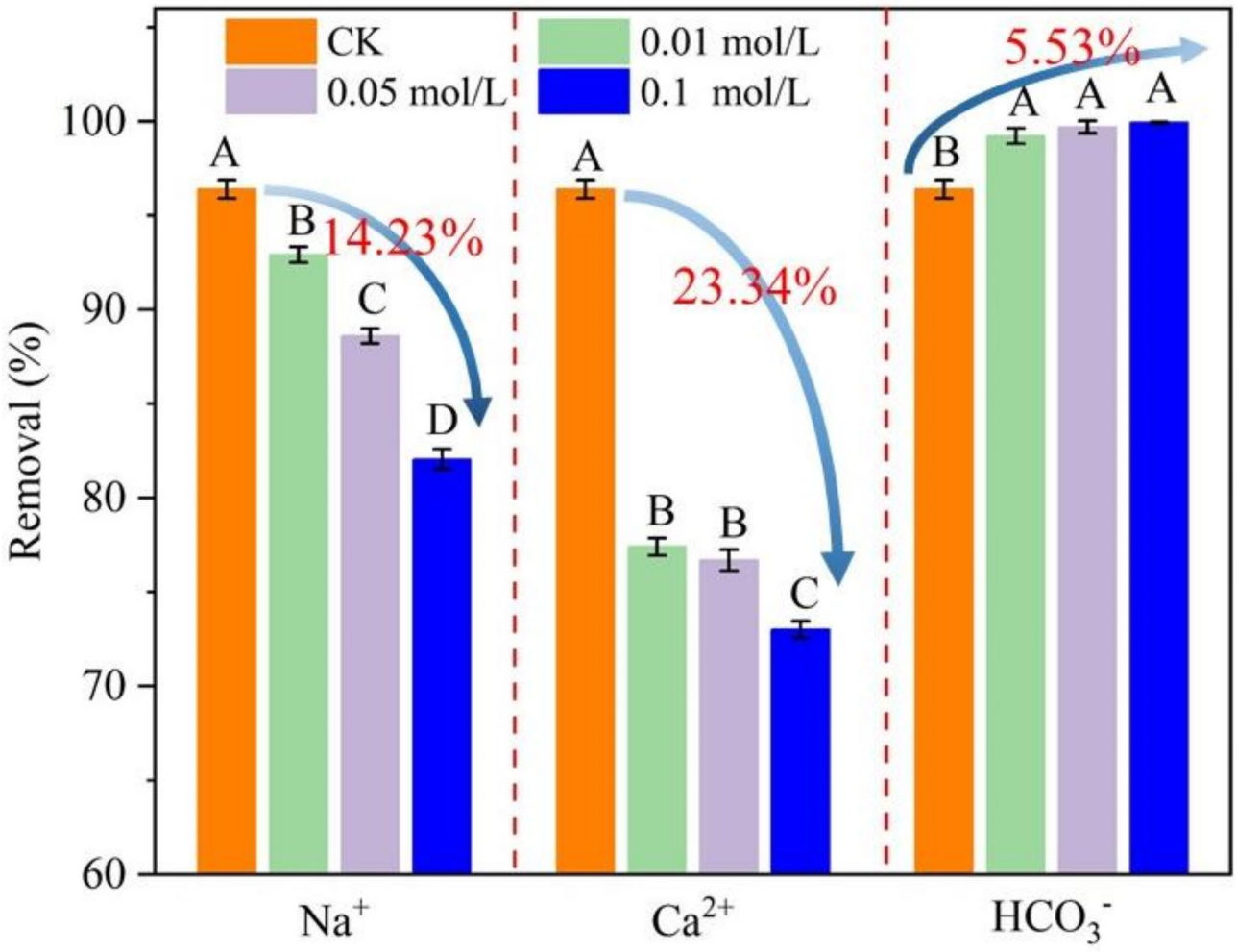

Fig. 18. Influence of the ionic strength on MB removal efficiency. Note: Different capital letters indicate significant differences within groups (P<0.01), using distilled water was the control group (CK).

in the previous tree, then output the final prediction results from all decision trees, finally, obtained a powerful prediction model.

Feature importance analysis

Although ML models showed the superior predictive ability, but they often was criticized as "black box", and it is difficult for explaining they internal decision making process. SHAP is a effective tool solve this problem, by assigning importance value of feature to interpret model output[84]. The key idea of SHAP based on shapley value from cooperative game theory, shapley value be used to distribute benefits among all participants by averaging, then, we incorporated this concept into machine learning model to calculate the contribution rate of each feature to prediction results[85]. Where, the positive and negative of SHAP value indicate positive correlation and negative correlation, respectively, the color from light blue to red indicates the degree of influence from small to large.

It can be see that (Fig. 22) the contact time is the biggest factor affecting the removal rate, this is consistent with the fact that adsorption process must be taken time to accumulate. The second factor is the ratio, there is evidence that modification can have both negative and positive effects on adsorbent performance, and that an optimal interval exists[86], therefore, the load ratio of modifier need special attention, this is confirmed by distribution of the SHAP value of ratio, and this result is consistent with our previous conclusion (Fig. 8). For pH, the high value are mainly concentrated on the right side, which may be related to the surface of SDMBC is negatively charged and while MB is a cationic pollutant, the negative charge on the SDMBC surface increased in the high pH solutions promotes MB adsorption[47]. Finally, concentration and temperature are the least influential input feature.

Figure 23 shows the SHAP value for each feature, which shows the importance of each feature for input variable. From this, the feature importance order is time > Ratio > pH > concentration > temperature, consistent with our results. The feature importance analysis provides valuable insights for studying adsorption behavior, landing a theoretical foundation for the subsequent optimization of experiment conditions and design of adsorbents.

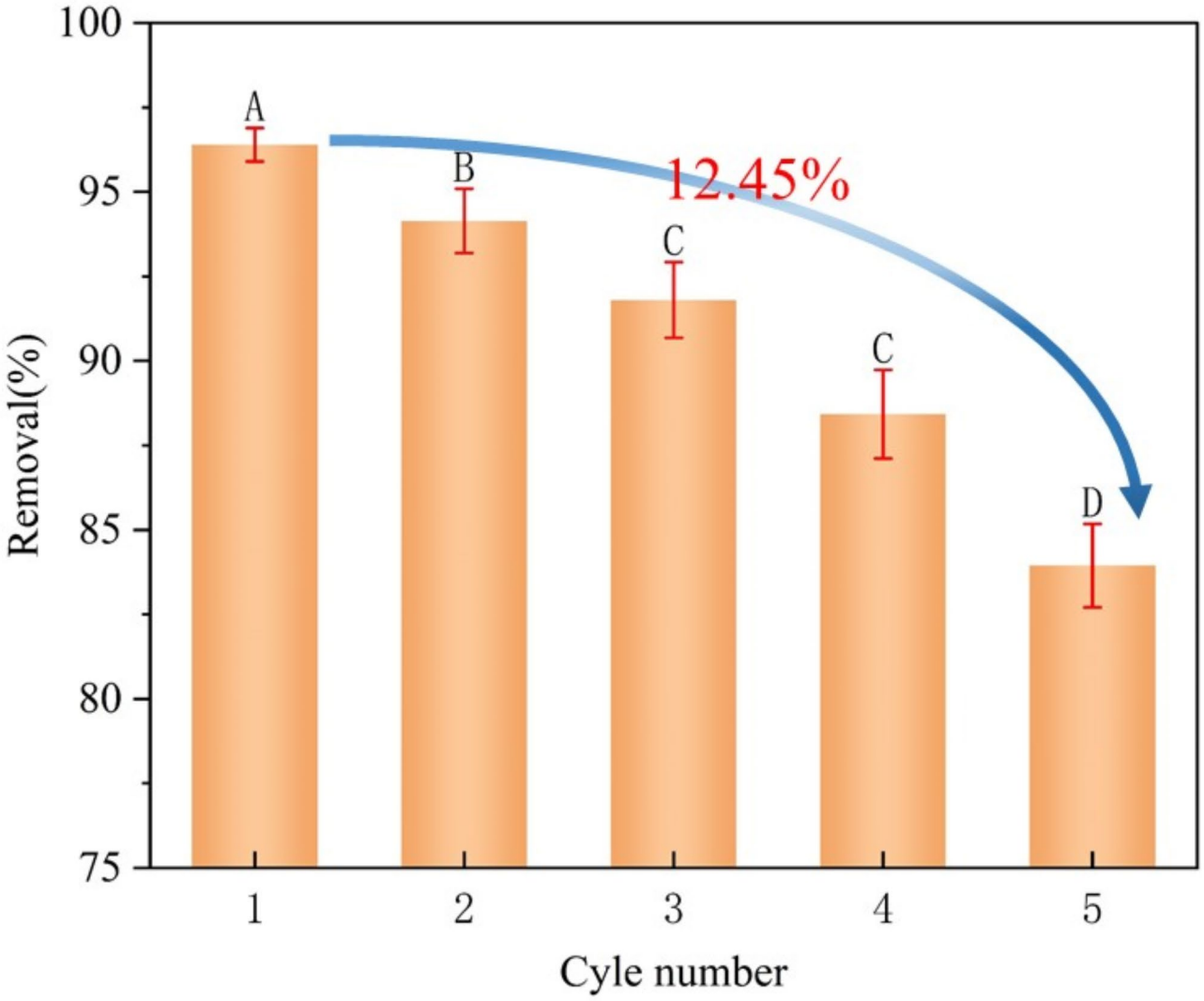

Fig. 19. Effect of reuse times of SDMBC on removal capacity, (kept above 85% original capacity after 5 recycling tests). Notes: Different capital letters indicate significant differences, $P<0.01$).

Materials	Purity	Price	Consumption	Cost
SDS	analytical grade	29.80 $/kg	369 g	10.99$
SAP	>99%	48.15 $/kg	160 g	7.7$
HNO_3	25%	8.9 $/L	0.4 L	3.56$
N_2	analytical grade	0.82 $/L	18 L	15.30$
Water	distilled water	0.04 $/L	50 L	2.00$
Electricity		100 kw·h	0.068 $/Kw·h	6.9$
Total				46.45$

Table 5. Cost estimates for production of 1Kg SDMBC.

Conclusion

In this work, a novel multifunction adsorbent SDMBC was successfully prepared by an simple and environmental friendly method, evaluated the performance of it through characterization techniques and batch experiment. Characterization results revealed that SDMBC have more well-developed layered structure, richer oxygen-containing functional groups and more amorphous structure compared to BC, which are closely related with improving its adsorption capacity. Batch adsorption results show that SDMBC presented a obvious improvement of adsorption performance compared with BC, which suggested the modification method was simple and efficient. The best modified effect was appeared when the concentration of SAP to SDS was 0.8 and 0.8 CMC, and

Materials	Cost ($/kg)
sigma-Aldrich-Norit	127.78$
sigma-Aldrich-Darco	205.05$
Thermo Fischer Scientific-Norit SA2	226.94$
Thermo Fischer Scientific-Norit A supra	553.83$
Thermo Fischer Scientific-Norit-Darco	176.38$
PAn/ZnO-PNC	65$
JS/ HSO-700	70$
This work	46.45$

Table 6. Comparative cost of SDMBC with some commercially available activated carbon.

Isotherm model	Parameters	Parameter value		
		298 K	303 K	308 K
Sips	q_m (mg/g)	208	160	245.71
	a_s	-43.82	-68.05	9.97
	B_s	58.56	-0.889	74.71
	R^2	0.241	0.957	0.633

Table 7. Sips isotherm model parameters for MB adsorption (Sips cannot describe well).

the adsorption capacity of MB, pb(II), Cd(II), BPA, and PNP onto SDMBC were 276.09, 130.23, 108.43, 125.27, 112.78 mg/g, respectively, importantly, SDMBC still maintains excellent adsorption capabilities in the binary competition adsorption. Subsequently, a comprehensive analysis of the adsorption behavior of MB on SDMBC, introduction the ML to construct prediction models and employ SHAP to to explain the model as interpreter, a cost analysis to conducted determine economic benefits of SDMBC. It was revealed that SDMBC can remain at a high level over a wide pH range, and less affected by ionic strength, the removal mechanism study indicates that the adsorption process is mainly controlled by hydrogen bond, electrostatic attraction and π-π interaction. The thermodynamic parameters confirmed that the adsorption of MB onto SDMBC was a spontaneous and endothermic process, a pseudo-second order model better fits the adsorption process, the Freundlich model was well described to the adsorption isotherm. After five recycling tests, kept above 85% original capacity, which indicates the SDMBC has effective recycling capabilities in practical application. Then, cost analysis was performed to confirm the cost of the SDMBC based on energy consumption and reagent costs, and the amount of SDMBC required for the adsorption of 99% of MB in a given volume of effluent was predicted. Finally, the XGBoost revealed the best prediction performance as compared other ML models, and SHAP analysis indicated that order relative importance feature is time > Ratio> pH > concentration > temperature. Overall, SDMBC shows great potential as a sustainable and effective of multifunctional adsorbent in the treatment of wastewater, builded prediction ML models have significance for optimizing adsorption efficiency in a sustainable way, this provide valuable insights for designing efficiency adsorbent, optimization of adsorption conditions.

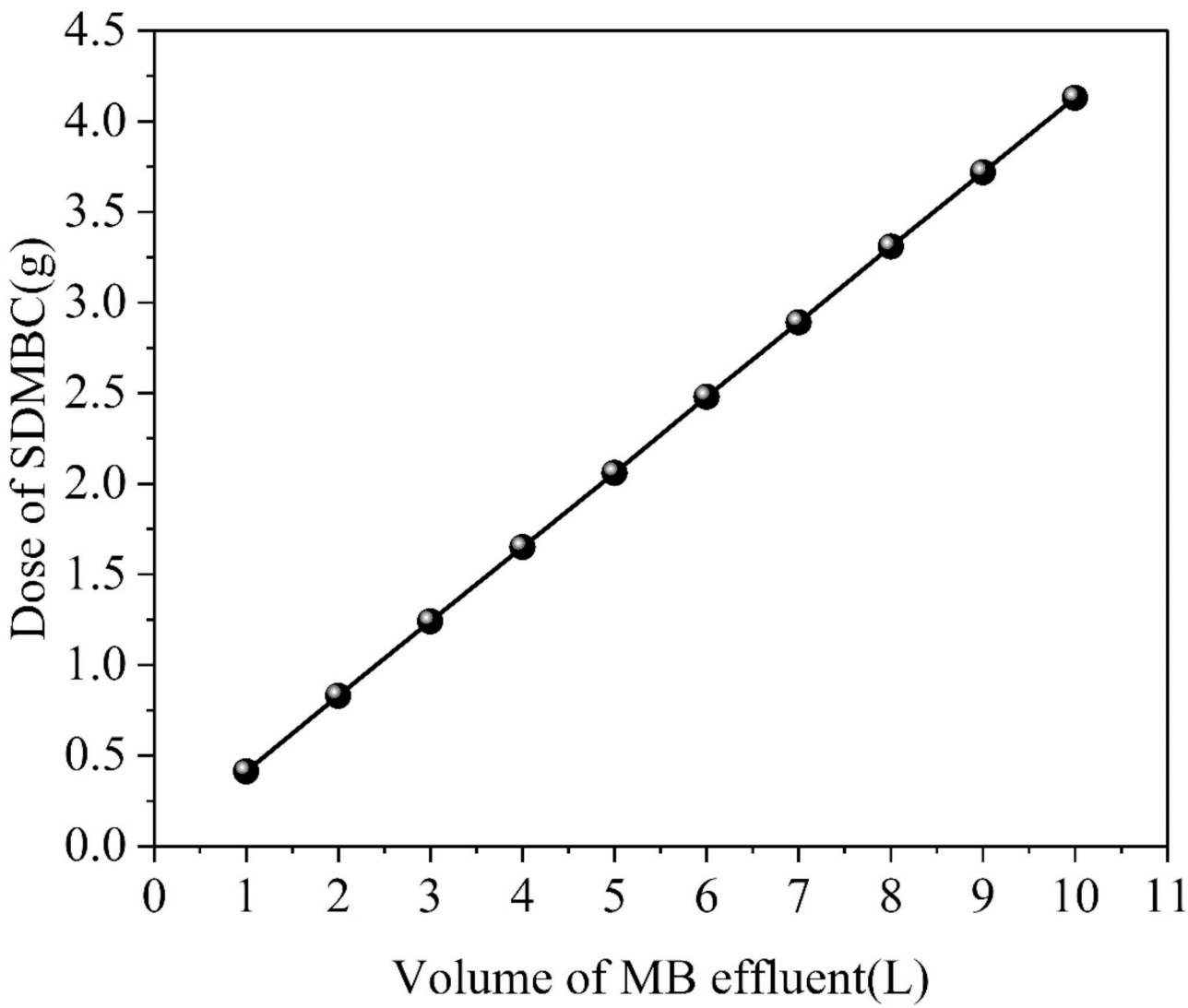

Fig. 20. Prediction of the amount of SDMBC required for the removal of MB in effluents of varying volume. (A dose of 4.13 g of SDMBC is required to eliminate 99% of 60 mg/L MB from a 10 L).

ML models	BP	CNN	SVR	PF	LsBoost	AbaBoost	XGBoost
Train R^2	0.967	0.979	0.963	0.834	0.991	0.894	0.998
Train MAE	2.827	2.172	2.818	6.420	1.340	1.747	0.547
Train RMSE	3.614	2.878	3.884	8.087	1.885	6.465	0.831
Test R^2	0.924	0.937	0.706	0.784	0.915	0.764	0.976
Test MAE	4.092	3.734	7.290	7.742	4.243	6.483	2.680
Test RMSE	5.221	4.100	10.580	9.069	5.693	9.434	3.433

Table 8. Comparison of parameters for seven ML models (XGBoost model has best performance).

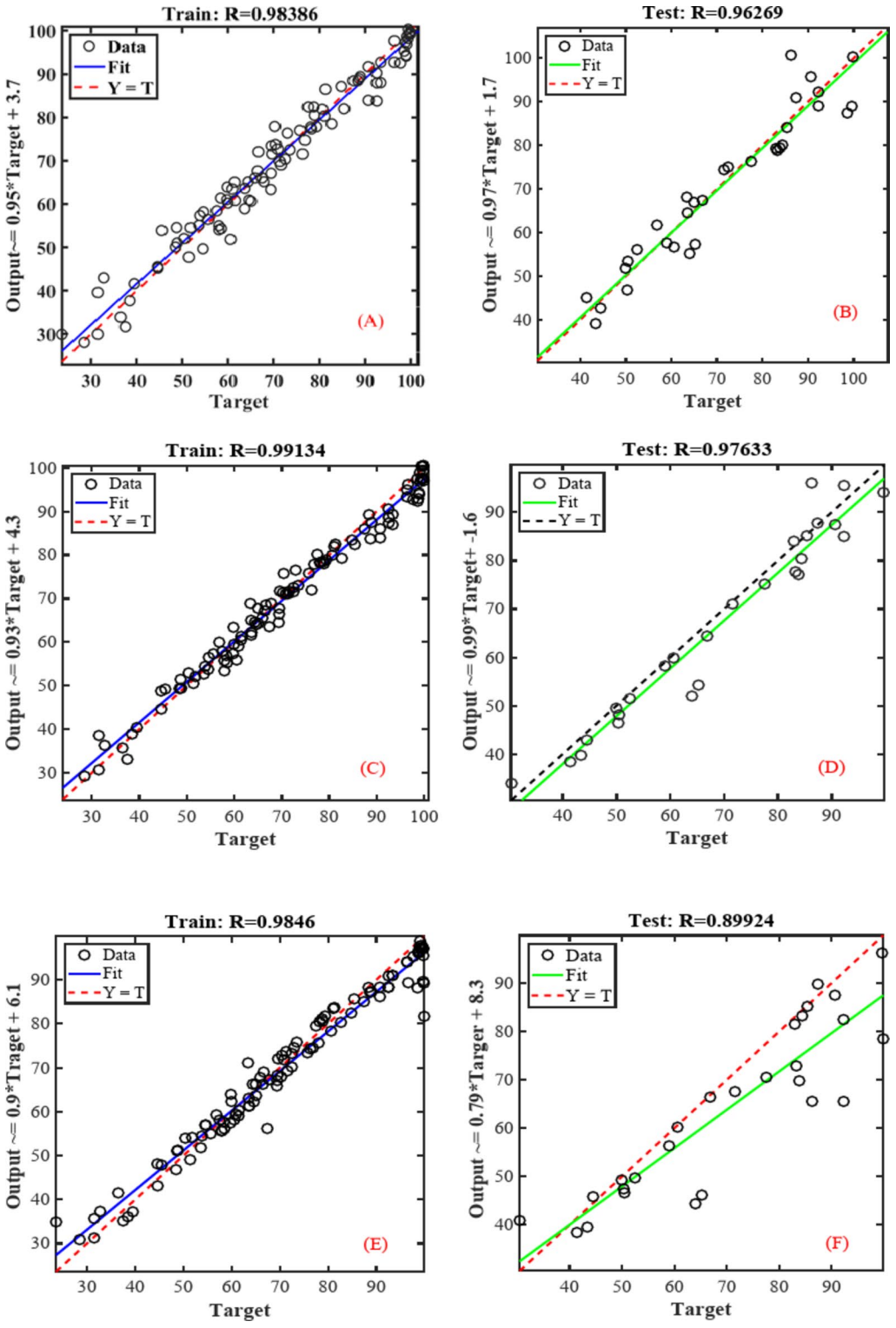

Fig. 21. Regression plots of ML for MB adsorption onto SDMBC, the solid line represents the ideal fit line, the dashed line (Y = T) represents the matched accuracy between output and actual data. BP (**A**,**B**); CNN (**C**,**D**); SVR (E, F); PF (G, H); LsBoost (I, J); AdaBoost (K, M); XGBoost (N, O). (The XGBoost model is the best-performing model).

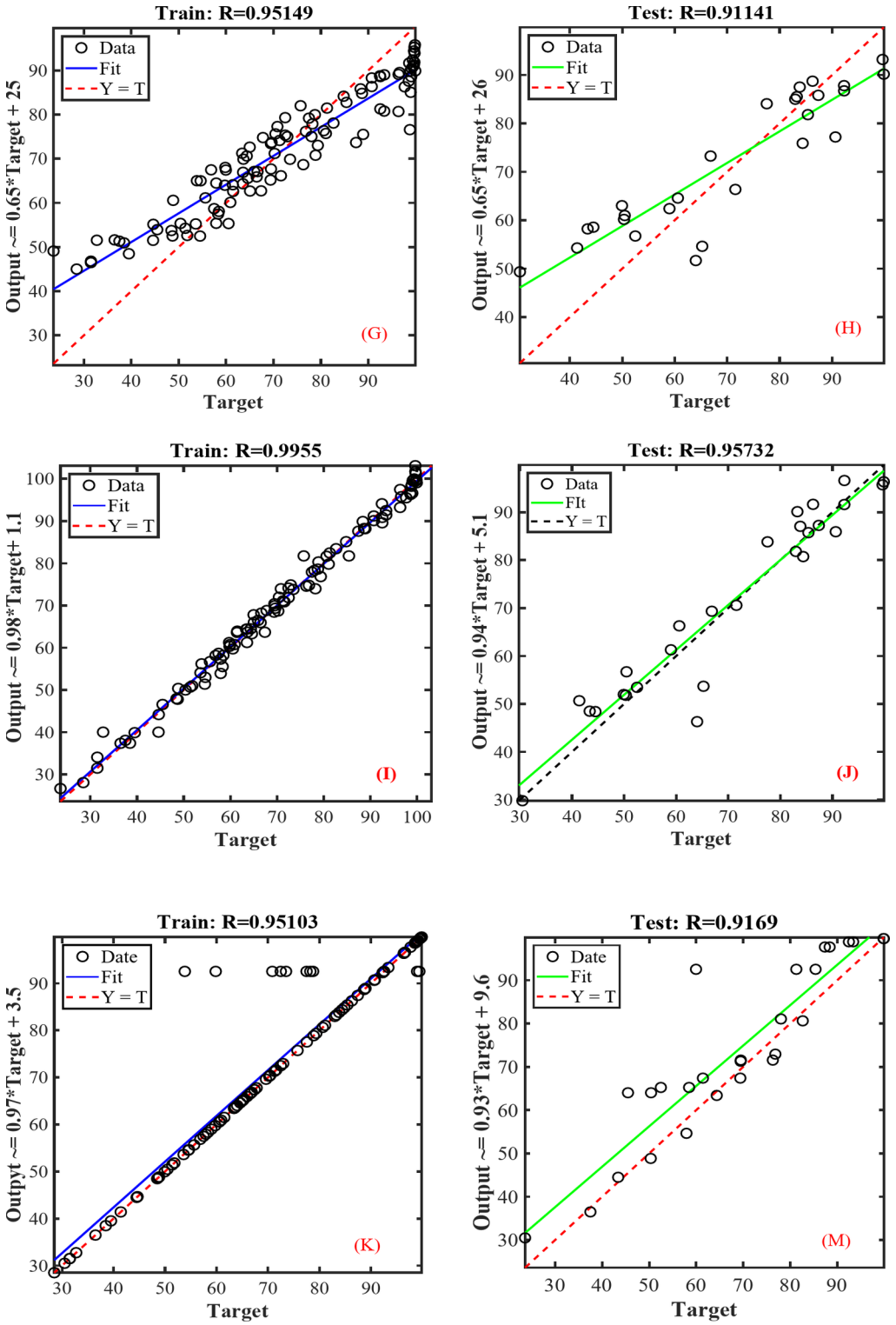

Figure 21. (continued)

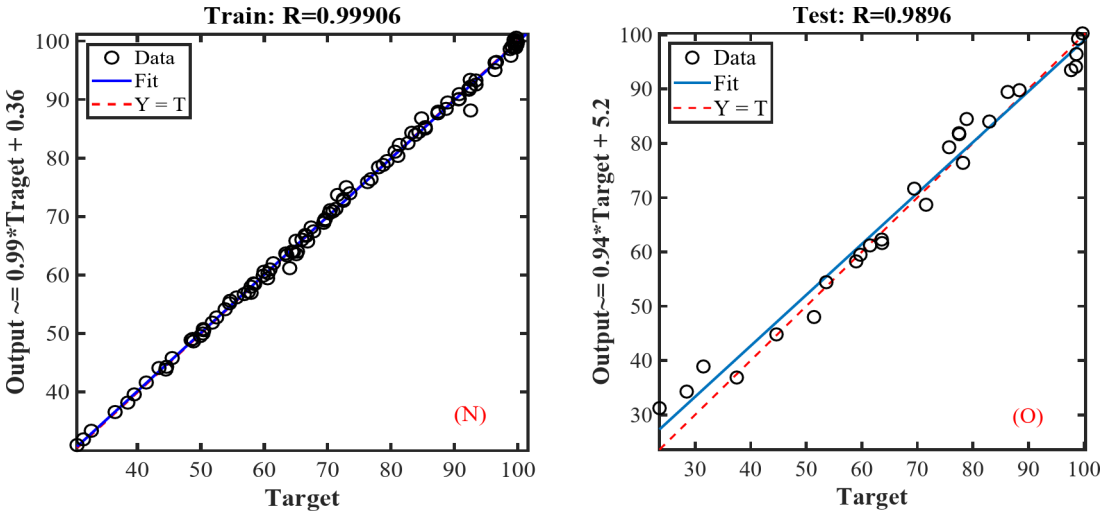

Figure 21. (continued)

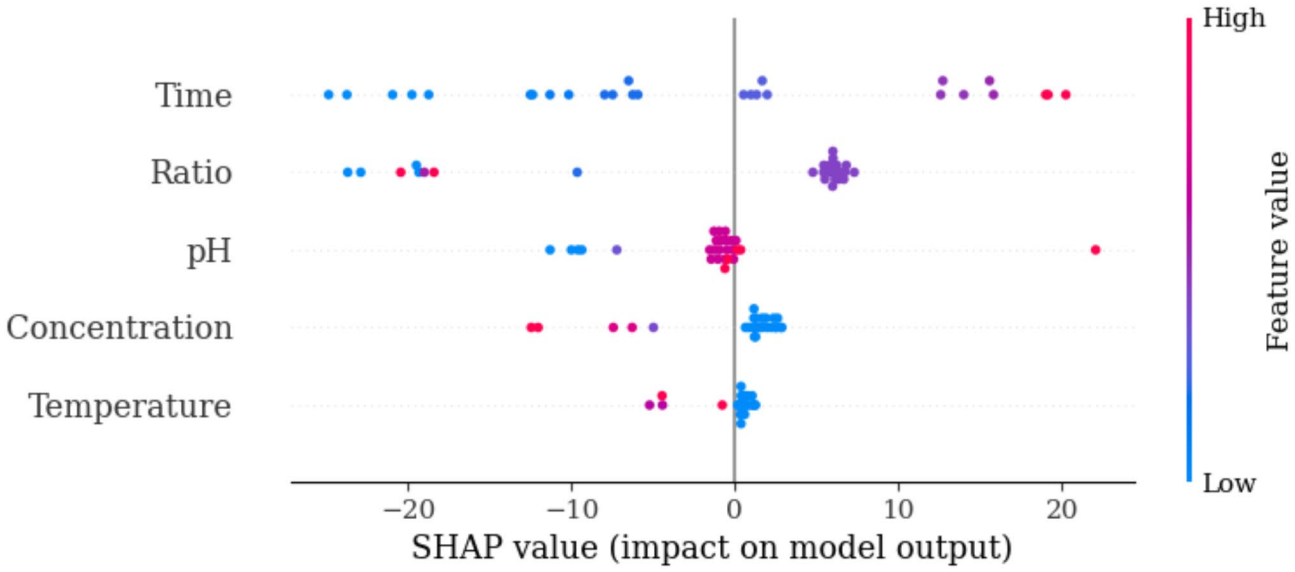

Fig. 22. SHAP values summary plot.

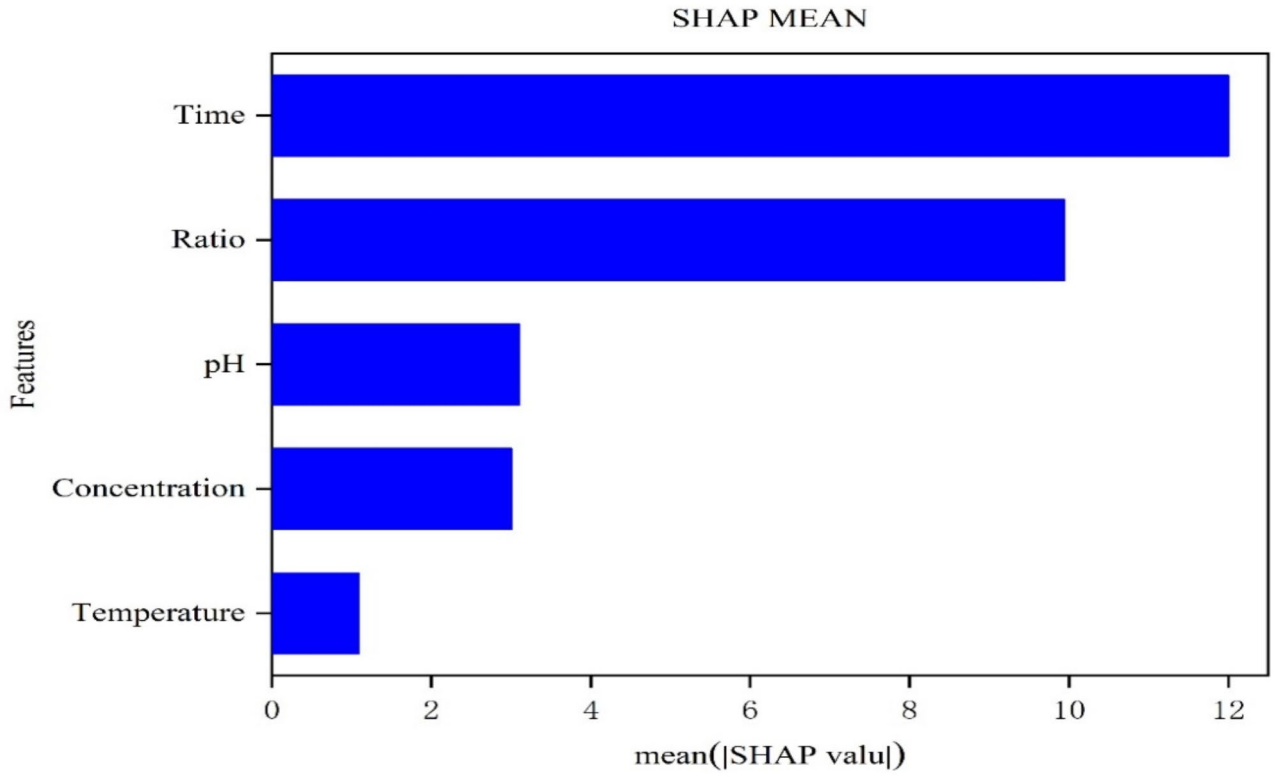

Fig. 23. SHAP output value of a single feature.

Data availability

Data is provided within the supplementary material 3. Should any raw data files be needed in another format, could be available from the corresponding author on reasonable request.

Received: 12 December 2024; Accepted: 19 February 2025
Published online: 28 February 2025

References

1. Tran, T. H. et al. Adsorption isotherms and kinetic modeling of methylene blue dye onto a carbonaceous hydrochar adsorbent derived from coffee husk waste. *Sci. Total Environ.* **725**, 138325. https://doi.org/10.1016/j.scitotenv.2020.138325 (2020).
2. El Messaoudi, N. et al. Recent developments in the synthesis of tetraethylenepentamine-based nanocomposites to eliminate heavy metal pollutants from wastewater through adsorption. *Bioresour. Technol. Rep.* **101982** https://doi.org/10.1016/j.biteb.2024.101982 (2024).
3. Chen, D. et al. Efficient removal of various coexisting organic pollutants in water based on β-cyclodextrin polymer modified flower-like Fe3O4 particles. *J. Colloid Interface Sci.* **589**, 217–228. https://doi.org/10.1016/j.jcis.2020.12.109 (2021).
4. Liu, J., Wang, X., Guo, S., Lu, A. & Jiang, H. Preparation of nitrogen doped magnetic carbon aerogel by sol–gel method combined with in-situ carbonization for simultaneous removal of p-nitrophenol and Pb (II). *Sep. Purif. Technol.* **130307** https://doi.org/10.1016/j.seppur.2024.130307 (2024).
5. McCarl, B. A., Peacocke, C., Chrisman, R., Kung, C. C. & Sands, R. D. Economics of Biochar production, utilization and greenhouse gas offsets. *Biochar Environ. Management: Sci. Technol.* **5**, 341–358 (2009).
6. Zhao, Y. et al. Modification of Garlic Peel by nitric acid and its application as a novel adsorbent for solid-phase extraction of quinolone antibiotics. *Chem. Eng. J.* **326**, 745–755. https://doi.org/10.1016/j.cej.2017.05.139 (2017).
7. Wang, Z. et al. Investigating the mechanisms of Biochar's removal of lead from solution. *Bioresour. Technol.* **177**, 308–317. https://doi.org/10.1016/j.biortech.2014.11.077 (2015).
8. Xue, G., Gao, M., Gu, Z., Luo, Z. & Hu, Z. The removal of p-nitrophenol from aqueous solutions by adsorption using gemini surfactants modified montmorillonites. *Chem. Eng. J.* **218**, 223–231. https://doi.org/10.1016/j.cej.2012.12.045 (2013).
9. Zhong, H. et al. Efficient adsorption removal of carbamazepine from water by dual-activator modified hydrochar. *Sep. Purif. Technol.* **353**, 128287. https://doi.org/10.1016/j.seppur.2024.128287 (2025).
10. Boumezough, Y., Arris, S., Carabineiro, S. A. & Viscusi, G. Optimized removal of methylene blue using chemically activated and thermally modified Opuntia ficus-indica Bioadsorbent: A response surface methodology approach. *Biomass Convers. Biorefin.* https://doi.org/10.1007/s13399-024-06370-y (2024).
11. Saleem, H., Pal, P., Haija, M. A. & Banat, F. Regeneration and reuse of bio-surfactant to produce colloidal gas aphrons for heavy metal ions removal using single and multistage cascade flotation. *J. Clean. Prod.* **217**, 493–502. https://doi.org/10.1016/j.jclepro.2019.01.216 (2019).
12. Zhang, Y. et al. Mechanisms and adsorption capacities of hydrogen peroxide modified ball milled Biochar for the removal of methylene blue from aqueous solutions. *Bioresour. Technol.* **337**, 125432. https://doi.org/10.1016/j.biortech.2021.125432 (2021).
13. Zhou, W., Yang, J., Lou, L. & Zhu, L. Solubilization properties of polycyclic aromatic hydrocarbons by Saponin, a plant-derived biosurfactant. *Environ. Pollut.* **159**, 1198–1204. https://doi.org/10.1016/j.envpol.2011.02.001 (2011).

14. Raji, F., Maghool, S., Shayesteh, H. & Rahbar-Kelishami, A. Effective adsorptive removal of Pb2 + ions from aqueous solution using functionalized agri-waste biosorbent: new green mediation via Seidlitzia rosmarinus extract. *Chemosphere* **363**, 142759. https://doi.org/10.1016/j.chemosphere.2024.142759 (2024).
15. Lamichhane, S., Krishna, K. B. & Sarukkalige, R. Surfactant-enhanced remediation of polycyclic aromatic hydrocarbons: a review. *J. Environ. Manage.* **199**, 46–61. https://doi.org/10.1016/j.jenvman.2017.05.037 (2017).
16. Yu, H., Zhu, L. & Zhou, W. Enhanced desorption and biodegradation of phenanthrene in soil–water systems with the presence of anionic–nonionic mixed surfactants. *J. Hazard. Mater.* **142**, 354–361. https://doi.org/10.1016/j.jhazmat.2006.08.028 (2007).
17. Shen, X. et al. Effects of mixed surfactants on the volatilization of naphthalene from aqueous solutions. *J. Hazard. Mater.* **140**, 187–193. https://doi.org/10.1016/j.jhazmat.2006.06.137 (2007).
18. Holland, P. & Rubingh, D. Nonideal multicomponent mixed micelle model. *J. Phys. Chem.* **87**, 1984–1990. https://doi.org/10.1021/j100234a030 (1983).
19. Largo, F. et al. Effective removal of toxic dye from wastewater via advanced modified magnetic sepiolite using combined surfactants SDS/CTAB/Fe3O4@ Sep: empirical and computational analysis studies. *J. Mol. Liq.* **125114** https://doi.org/10.1016/j.molliq.2024.125114 (2024).
20. Li, H. et al. Construction and characterization of sodium alginate/polyvinyl alcohol double-network hydrogel beads with surfactant-tailored adsorption capabilities for efficient Tetracycline hydrochloride removal. *Int. J. Biol. Macromol.* **280**, 135879. https://doi.org/10.1016/j.ijbiomac.2024.135879 (2024).
21. Pan, X. et al. Functionalization of sawdust Biochar using Mg-Fe-LDH and sodium Dodecyl sulfonate enhanced its stability and immobilization capacity for cd and Pb in contaminated water and soil. *Biochar* **7**, 16. https://doi.org/10.1007/s42773-024-00401-7 (2025).
22. Chen, C. et al. Extraction and purification of saponins from Sapindus mukorossi. *New J. Chem.* **45**, 952–960. https://doi.org/10.1039/D0NJ04047A (2021).
23. Zhang, N. et al. Efficient remediation of soils contaminated with petroleum hydrocarbons using sustainable plant-derived surfactants. *Environ. Pollut.* **337**, 122566. https://doi.org/10.1016/j.envpol.2023.122566 (2023).
24. Nirmala, N. et al. Removal of toxic metals from wastewater environment by graphene-based composites: A review on isotherm and kinetic models, recent trends, challenges and future directions. *Sci. Total Environ.* **840**, 156564. https://doi.org/10.1016/j.scitotenv.2022.156564 (2022).
25. Tang, J., He, J., Liu, T. & Xin, X. Removal of heavy metals with sequential sludge washing techniques using Saponin: optimization conditions, kinetics, removal effectiveness, binding intensity, mobility and mechanism. *RSC Adv.* **7**, 33385–33401. https://doi.org/10.1039/C7RA04284A (2017).
26. Mondal, M. H., Malik, S., Garain, A., Mandal, S. & Saha, B. Extraction of natural surfactant saponin from soapnut (Sapindus mukorossi) and its utilization in the remediation of hexavalent chromium from contaminated water. *Tenside Surfactants Detergents*. **54**, 519–529. https://doi.org/10.3139/113.110523 (2017).
27. Gao, L. et al. Behavior and distribution of heavy metals including rare earth elements, thorium, and uranium in sludge from industry water treatment plant and recovery method of metals by biosurfactants application. *Bioinorg. Chem. Appl.* 173819 (2012). https://doi.org/10.1155/2012/173819 (2012).
28. Huang, W. & Liu, Z. Biosorption of cd (II)/Pb (II) from aqueous solution by biosurfactant-producing bacteria: isotherm kinetic characteristic and mechanism studies. *Colloids Surf. B.* **105**, 113–119. https://doi.org/10.1016/j.colsurfb.2012.12.040 (2013).
29. Upadhyay, S. & Hari, O. Spectrophotometric and conductometric study of the interaction of saponin with chromium (VI) and lead (II). *Int. J. Environ. Sci. Technol.* **16**, 7997–8004. https://doi.org/10.1007/s13762-019-02210-z (2019).
30. Al-Kadhi, N. S., Al-Senani, G. M., Saad, F. A., Munshi, A. M. & Abdelrahman, E. A. Modification of nickel ferrite nanoparticles by sodium docusate surfactant for superior crystal Violet dye removal from aqueous solutions. *Sci. Rep.* **14**, 27973 (2024).
31. Momina, M., Qurtulen, Q., Shahraki, H. S., Ahmad, A. & Zaheer, Z. Machine learning approaches to predict adsorption performance of sugarcane derived-carbon dot – based composite in the removal of dyes. *Sep. Purif. Technol.* **351**, 127937. https://doi.org/10.1016/j.seppur.2024.127937 (2024).
32. Mahmoud, A. E. D., Ali, R. & Fawzy, M. Insights into Levofloxacin adsorption with machine learning models using nano-composite hydrochars. *Chemosphere* **355**, 141746. https://doi.org/10.1016/j.chemosphere.2024.141746 (2024).
33. Lyu, H. et al. Machine learning-driven prediction of phosphorus adsorption capacity of Biochar: insights for adsorbent design and process optimization. *J. Environ. Manage.* **369**, 122405. https://doi.org/10.1016/j.jenvman.2024.122405 (2024).
34. Zhu, X. et al. Machine learning for the selection of carbon-based materials for Tetracycline and sulfamethoxazole adsorption. *Chem. Eng. J.* **406**, 126782. https://doi.org/10.1016/j.cej.2020.126782 (2021).
35. Chen, Y., Wang, S., Kang, L. & Kong, L. Enhanced adsorption of Ni (ii) using ATP/PPy/SDS composite. *RSC Adv.* **6**, 11735–11741. https://doi.org/10.1039/C5RA21407F (2016).
36. Lv, B. W., Xu, H., Guo, J. Z., Bai, L. Q. & Li, B. Efficient adsorption of methylene blue on carboxylate-rich hydrochar prepared by one-step hydrothermal carbonization of bamboo and acrylic acid with ammonium persulphate. *J. Hazard. Mater.* **421**, 126741. https://doi.org/10.1016/j.jhazmat.2021.126741 (2022).
37. Yin, G. et al. Novel Fe-Mn binary oxide-biochar as an adsorbent for removing cd (II) from aqueous solutions. *Chem. Eng. J.* **389**, 124465. https://doi.org/10.1016/j.cej.2020.124465 (2020).
38. Shakya, A., Vithanage, M. & Agarwal, T. Influence of pyrolysis temperature on Biochar properties and cr (VI) adsorption from water with groundnut shell Biochars: mechanistic approach. *Environ. Res.* **215**, 114243 (2022).
39. Mallick, A., Mukhopadhyay, M. & Ash, S. Synthesis, characterization and performance evaluation of a solid acid catalyst prepared from coconut shell for hydrolyzing pretreated Acacia nilotica Heartwood. *J. Institution Eng. (India): Ser. E.* **101**, 69–76. https://doi.org/10.1007/s40034-019-00153-1 (2020).
40. Zhang, K., Dwivedi, V., Chi, C. & Wu, J. Graphene oxide/ferric hydroxide composites for efficient arsenate removal from drinking water. *J. Hazard. Mater.* **182**, 162–168. https://doi.org/10.1007/s40034-019-00153-1 (2010).
41. Anbia, M. & Amirmahmoodi, S. Removal of hg (II) and Mn (II) from aqueous solution using nanoporous carbon impregnated with surfactants. *Arab. J. Chem.* **9**, 319–S325. https://doi.org/10.1016/j.arabjc.2011.04.004 (2016).
42. Hong, K. J., Tokunaga, S. & Kajiuchi, T. Evaluation of remediation process with plant-derived biosurfactant for recovery of heavy metals from contaminated soils. *Chemosphere* **49**, 379–387. https://doi.org/10.1016/S0045-6535(02)00321-1 (2002).
43. Zhao, X., Wang, X. & Lou, T. Preparation of fibrous Chitosan/sodium alginate composite foams for the adsorption of cationic and anionic dyes. *J. Hazard. Mater.* **403**, 124054. https://doi.org/10.1016/j.jhazmat.2020.124054 (2021).
44. Liu, W. et al. Cross-linking of Poly (dimethylaminoethyl methacrylate) by phytic acid: pH-responsive adsorbent for high-efficiency removal of cationic and anionic dyes. *RSC Adv.* **10**, 4232–4242. https://doi.org/10.1039/C9RA09391E (2020).
45. Alghamdi, W. M. & El Mannoubi, I. Investigation of seeds and peels of Citrullus colocynthis as efficient natural adsorbent for methylene blue dye. *Processes* **9**, 1279. https://doi.org/10.3390/pr9081279 (2021).
46. Inyinbor, A., Adekola, F. & Olatunji, G. A. Kinetics and isothermal modeling of liquid phase adsorption of Rhodamine B onto Urea modified Raphia Hookerie epicarp. *Appl. Water Sci.* **7**, 3257–3266. https://doi.org/10.1007/s13201-016-0471-7 (2017).
47. Amran, F. & Zaini, M. A. A. Sodium hydroxide-activated Casuarina empty fruit: isotherm, kinetics and thermodynamics of methylene blue and congo red adsorption. *Environ. Technol. Innov.* **23**, 101727. https://doi.org/10.1016/j.eti.2021.101727 (2021).
48. Lin, C. et al. A study on adsorption of cr (VI) by modified rice straw: characteristics, performances and mechanism. *J. Clean. Prod.* **196**, 626–634. https://doi.org/10.1016/j.jclepro.2018.05.279 (2018).

49. Georgin, J., Franco, D. S. P., Dehmani, Y. & Nguyen-Tri, P. El Messaoudi, N. Current status of advancement in remediation technologies for the toxic metal mercury in the environment: A critical review. *Sci. Total Environ.* **174501** https://doi.org/10.1016/j.scitotenv.2024.174501 (2024).
50. Zhao, Y. et al. Insights into enhanced adsorptive removal of Rhodamine B by different chemically modified Garlic peels: comparison, kinetics, isotherms, thermodynamics and mechanism. *J. Mol. Liq.* **293**, 111516. https://doi.org/10.1016/j.molliq.2019.111516 (2019).
51. Wang, Y. et al. Removal of Pb (II) and methylene blue from aqueous solution by magnetic hydroxyapatite-immobilized oxidized multi-walled carbon nanotubes. *J. Colloid Interface Sci.* **494**, 380–388. https://doi.org/10.1016/j.jcis.2017.01.105 (2017).
52. Xin, W. et al. Removal of bisphenol A (BPA) by fermented sludge-derived granular Biochar from template-like method: from batch experiment to continuous operation. *Process Saf. Environ. Prot.* **168**, 239–247. https://doi.org/10.1016/j.psep.2022.10.002 (2022).
53. Chaturvedi, M. et al. Composites of sodium alginate based-Functional materials towards sustainable adsorption of benzene phenol derivatives-Bisphenol A/Triclosan. *Environ. Res.* **255**, 119192. https://doi.org/10.1016/j.envres.2024.119192 (2024).
54. Yang, Z., Wei, C., Chai, Y., Zhang, J. & Ji, H. Dibenzo-18-crown-6-functionalized organic nanotubes for the synergistic adsorption of dyes and phenols from aqueous solutions. *J. Water Process. Eng.* **50**, 103213. https://doi.org/10.1016/j.jwpe.2022.103213 (2022).
55. Liu, L., Deng, G. & Shi, X. Adsorption characteristics and mechanism of p-nitrophenol by pine sawdust Biochar samples produced at different pyrolysis temperatures. *Sci. Rep.* **10**, 5149. https://doi.org/10.1038/s41598-020-62059-y (2020).
56. Chen, H., Zhang, Y., Li, J., Zhang, P. & Liu, N. Preparation of pickling-reheating activated alfalfa Biochar with high adsorption efficiency for p-nitrophenol: characterization, adsorption behavior, and mechanism. *Environ. Sci. Pollut. Res.* **26**, 15300–15313. https://doi.org/10.1007/s11356-019-04862-3 (2019).
57. Xu, H. et al. Enhanced removal efficiency of Cd2 + and Pb2 + from aqueous solution by H3PO4–modified tea branch Biochar: characterization, adsorption performance and mechanism. *J. Environ. Chem. Eng.* **12**, 112183. https://doi.org/10.1016/j.jece.2024.112183 (2024).
58. Zhu, X. et al. Green modification of Biochar with Poly (aspartic acid) enhances the remediation of cd and Pb in water and soil. *J. Environ. Manage.* **370**, 122642. https://doi.org/10.1016/j.jenvman.2024.122642 (2024).
59. Zhou, Z., Huang, L., Wang, H. & Chen, Y. Efficient removal of cadmium and lead in water by using nano-manganese oxide-loaded hydrochloric acid pretreated Biochar. *J. Environ. Chem. Eng.* **12**, 113548. https://doi.org/10.1016/j.jece.2024.113548 (2024).
60. Chen, D., Ding, Z., Zou, L., Wang, Y. & Zeng, X. Composite of hydrolyzed PAN and β-Cyclodextrin forms a nanofiber membrane with an excellent removal effect on various cationic dyes and copper ions. *Langmuir* https://doi.org/10.1021/acs.langmuir.4c03397 (2024).
61. Wang, B., Ma, Y., Cao, P., Tang, X. & Xin, J. Ball milling and magnetic modification boosted methylene blue removal by Biochar obtained from water hyacinth: efficiency, mechanism, and application. *Molecules* **29**, 5141. https://doi.org/10.3390/molecules292151415141 (2024).
62. Saad, E. M., Wagdy, M. & Orabi, A. S. Advanced nano modification of ecofriendly glauconite clay for high efficiency methylene blue dye adsorption. *Sci. Rep.* **14**, 23614. https://doi.org/10.1038/s41598-024-71979-y (2024).
63. Tran, H. N., You, S. J. & Chao, H. P. Insight into adsorption mechanism of cationic dye onto agricultural residues-derived hydrochars: negligible role of π-π interaction. *Korean J. Chem. Eng.* **34**, 1708–1720. https://doi.org/10.1007/s11814-017-0056-7 (2017).
64. Ma, H., Xu, Z., Wang, W., Gao, X. & Ma, H. Adsorption and regeneration of leaf-based Biochar for p-nitrophenol adsorption from aqueous solution. *RSC Adv.* **9**, 39282–39293. https://doi.org/10.1039/C9RA07943B (2019).
65. Katibi, K. K. et al. Unlocking the potential of magnetic Biochar in wastewater purification: a review on the removal of bisphenol A from aqueous solution. *Environ. Monit. Assess.* **196**, 492. https://doi.org/10.1007/s10661-024-12574-6 (2024).
66. Li, Z., Hu, C., Hu, Z., Fu, Y. & Chen, Z. Facile synthesis of novel multifunctional β-cyclodextrin microporous organic network and application in efficient removal of bisphenol A from water. *Carbohydr. Polym.* **276**, 118786. https://doi.org/10.1016/j.carbpol.2021.118786 (2022).
67. Meneses, I. P., Novaes, S. D., Dezotti, R. S., Oliveira, P. V. & Petri, D. F. CTAB-modified carboxymethyl cellulose/bagasse cryogels for the efficient removal of bisphenol A, methylene blue and cr (VI) ions: batch and column adsorption studies. *J. Hazard. Mater.* **421**, 126804. https://doi.org/10.1016/j.jhazmat.2021.126804 (2022).
68. Hemine, K., Łukasik, N., Gazda, M. & Nowak, I. β-cyclodextrin-containing polymer based on renewable cellulose resources for effective removal of ionic and non-ionic toxic organic pollutants from water. *J. Hazard. Mater.* **418**, 126286. https://doi.org/10.1016/j.jhazmat.2021.126286 (2021).
69. El Messaoudi, N. et al. Comprehensive analytical review of heavy metal removal efficiency using agricultural solid waste-based bionanocomposites. *Nano-Struct Nano-Objects*. **38**, 101220. https://doi.org/10.1016/j.nanoso.2024.101220 (2024).
70. Miyah, Y. et al. A comprehensive review of β-cyclodextrin polymer nanocomposites exploration for heavy metal removal from wastewater. *Carbohydr. Polym.* **122981** https://doi.org/10.1016/j.carbpol.2024.122981 (2024).
71. Verma, L. & Singh, J. Synthesis of novel Biochar from waste plant litter biomass for the removal of arsenic (III and V) from aqueous solution: A mechanism characterization, kinetics and thermodynamics. *J. Environ. Manage.* **248**, 109235. https://doi.org/10.1016/j.jenvman.2019.07.006 (2019).
72. Sun, D. et al. Qualitative and quantitative investigation on adsorption mechanisms of cd (II) on modified Biochar derived from co-pyrolysis of straw and sodium phytate. *Sci. Total Environ.* **829**, 154599. https://doi.org/10.1016/j.scitotenv.2022.154599 (2022).
73. Liu, Y. et al. β-Cyclodextrin-based Hollow nanoparticles with excellent adsorption performance towards organic and inorganic pollutants. *Nanoscale* **11**, 18653–18661. https://doi.org/10.1039/C9NR07342F (2019).
74. Shen, Y., Ni, W. X. & Li, B. Porous organic polymer synthesized by green diazo-coupling reaction for adsorptive removal of methylene blue. *ACS Omega*. **6**, 3202–3208. https://doi.org/10.1021/acsomega.0c05634 (2021).
75. Bian, G. et al. Early development and functional properties of tryptase/chymase double-positive mast cells from human pluripotent stem cells. *J. Mol. Cell Biol.* **13**, 104–115. https://doi.org/10.1093/jmcb/mjaa059 (2021).
76. Li, B., Guo, J., Lv, K. & Fan, J. Adsorption of methylene blue and cd (II) onto maleylated modified hydrochar from water. *Environ. Pollut.* **254**, 113014. https://doi.org/10.1016/j.envpol.2019.113014 (2019).
77. Wu, Z. et al. Enhanced adsorptive removal of p-nitrophenol from water by aluminum metal–organic framework/reduced graphene oxide composite. *Sci. Rep.* **6**, 25638. https://doi.org/10.1038/srep25638 (2016).
78. Bo, L., Gao, F., Bian, Y., Liu, Z. & Dai, Y. A novel adsorbent auricularia auricular for the removal of methylene blue from aqueous solution: isotherm and kinetics studies. *Environ. Technol. Innov.* **23**, 101576. https://doi.org/10.1016/j.eti.2021.101576 (2021).
79. Mosoarca, G., Vancea, C., Popa, S., Dan, M. & Boran, S. The use of Bilberry leaves (Vaccinium myrtillus L.) as an efficient adsorbent for cationic dye removal from aqueous solutions. *Polymers* **14**, 978. https://doi.org/10.3390/polym14050978 (2022).
80. Deb, A., Debnath, A., Bhattacharjee, N. & Saha, B. Ultrasonically enhanced dye removal using conducting polymer functionalised ZnO nanocomposite at near neutral pH: kinetic study, isotherm modelling and adsorbent cost analysis. *Int. J. Environ. Anal. Chem.* **102**, 8055–8074. https://doi.org/10.1080/03067319.2020.1843649 (2022).
81. Dzoujo, H. T. et al. Synthesis of Pozzolan and sugarcane Bagasse derived geopolymer-biochar composites for methylene blue sequestration from aqueous medium. *J. Environ. Manage.* **318**, 115533. https://doi.org/10.1016/j.jenvman.2022.115533 (2022).
82. Shikuku, V. O. & Jemutai-Kimosop, S. Efficient removal of sulfamethoxazole onto sugarcane bagasse-derived Biochar: two and three-parameter isotherms, kinetics and thermodynamics. *S Afr. J. Chem.* **73**, 111–119 (2020).
83. Oviedo, L. R., Oviedo, V. R., Nora, D., da Silva, W. L. & L. D. & Adsorption of organic dyes onto nanozeolites: A machine learning study. *Sep. Purif. Technol.* **315**, 123712. https://doi.org/10.1016/j.seppur.2023.123712 (2023).

84. Zhao, S., Chen, K., Xiong, B., Guo, C. & Dang, Z. Prediction of adsorption of metal cations by clay minerals using machine learning. *Sci. Total Environ.* **924**, 171733. https://doi.org/10.1016/j.scitotenv.2024.171733 (2024).
85. Chen, L. et al. Predicting cd (II) adsorption capacity of Biochar materials using typical machine learning models for effective remediation of aquatic environments. *Sci. Total Environ.* **173955** https://doi.org/10.1016/j.scitotenv.2024.173955 (2024).
86. Kuang, Y., Zhang, X. & Zhou, S. Adsorption of methylene blue in water onto activated carbon by surfactant modification. *Water* **12**, 587. https://doi.org/10.3390/w12020587 (2020).

Acknowledgements

Thanks for the technical and experimental equipment support provided by Key Laboratory for Forest Resources Conservation and Utilization in the Southwest Mountains of China Ministry of Education.

Author contributions

K. T conceived and designed of the work, and he also performed experiments, collected data, analysis data, and wrote the manuscript. C. P. L participated in the study design, sample collection and discussions on the results. L. C. W participated in the preparation of study protocol and reviewed the manuscript. H. M. L provided technical support. All authors read and approved the final manuscript.

Funding

This research was funded by the Research on key technologies for efficient cultivation of important industrial raw material forests (2023YFD2201103).

Declarations

Competing interests

The authors declare no competing interests.

Additional information

Supplementary Information The online version contains supplementary material available at https://doi.org/10.1038/s41598-025-91229-z.

Correspondence and requests for materials should be addressed to L.W.